FUTURE OF AUSTRALIAN RAIL TRACKS CAPTURING HIGHER SPEEDS WITH HEAVIER FREIGHT

Buddhima Indraratna[1], Sanjay Nimbalkar[2] and Cholachat Rujikiatkamjorn[3]
[1]Professor and Research Director, [2]Research Fellow, [3]Senior Lecturer, Centre for Geomechanics and Railway Engineering; ARC Centre of Excellence for Geotechnical Science and Engineering, University of Wollongong, Wollongong, Australia

ABSTRACT

In Australia, quicker and more cost effective commuter and freight transports are essential to cater for the needs of travel demand and supply chains in the mining and agriculture sectors. Such development in coastal areas would necessitate the use of ground improvement techniques in response to environmental legislation and requirements for improved performance and sustainability. In coastal Australia the high cost of track maintenance is the main issue due to poor drainage of soft coastal soils, ballast degradation, fouling (e.g. coal and subgrade soil), differential settlement of track, pumping of subgrade soils and track misalignment due to excessive lateral movements. Hundreds of millions of dollars are spent each year on the construction and maintenance of rail tracks and the existing technical specifications, standards and design are often unable to address these problems. With increased train speeds, the capacity of the track is often inadequate unless more resilient tracks are designed to withstand the substantially increased vibration and cyclic and impact loads. The optimum use of maintenance funds is a challenging task due to the absence of comprehensive methods to predict track longevity even on terrain where the properties of the soils are well established. Until today, the vast majority of Australian track designs have considered ballast and structural fill as elastic granular media, and thus the designers have adopted predominantly empirical methods where true cyclic loading patterns and the onset of plasticity and degradation of track materials are ignored. In many European countries and some parts of Southeast Asia, especially among high speed rail networks, track vibrations are serious concerns. The mechanisms of ballast degradation and deformation, the need for effective track confinement, understanding the interface behaviour and the imperative need for flood protection, time dependent drainage and filtration properties of track materials requires further research to improve the existing design guidelines and Australian Standards for future high speed commuter and heavier freight trains. Field studies on instrumented tracks at Bulli (near Wollongong) and Singleton (near Newcastle) supported by RailCorp and ARTC, were carried out to measure the *in situ* stresses and deformation of ballast embankments. The application of prefabricated vertical drains (PVDs) to stabilise soft subgrade soils was introduced for the first time in Australia to improve the overall track stability in Sandgate (near Newcastle). The effectiveness of using PVDs was observed through field measurements and finite element analyses. In this keynote paper, the current state-of-the-art knowledge of rail track geotechnology in Australia and around the world is discussed. The paper focuses on primary research and development of new design and construction concepts for enhanced track performance, highlighting examples of innovations from theory to practice. Through case studies, the paper also introduces predictive and design tools for practitioners via user-friendly approaches.

1 INTRODUCTION

Railways play an integral role in multi-modal freight transport. There is great potential for expanding the freight rail system in Australia, but increasing the traffic tonnages and speed are limited by the conditions of the track and maintenance costs associated with its subsequent degradation. The large lateral deformations of ballast due to insufficient track confinement, fouling of ballast by coal from freight trains, soft formation soils (clay pumping) and as well as ballast breakage, are the primary causes of track deterioration. Quarrying for fresh ballast in spite of stringent environment controls, stockpiling of used ballast with little demand for recycling, and routine interruption of traffic to repair tracks have been instrumental in the allocation of significant research funds to improve ballasted rail tracks in Australia, North America, Western Europe, and Southeast Asia. The main objectives of Australian Rail are to cater for the mining and agriculture sectors (meeting the demands of the supply chain), and provide quicker and more cost effective commuter expectations, but several geotechnical problems in the populated coastal areas pose significant problems. The constraints of restricted space, tight construction schedules, environmental and safety issues, maintenance costs, and the longevity of earth structures, have continued to demand unfailing innovation in the design and construction of essential infrastructure on soft clays.

Rail tracks undergo millions of loading cycles of varying magnitudes and frequencies during their service life. The transfer of moving wheel loads at higher speeds (> 150 km/h) results in a significant increase in track damage because the quasi-static response at relatively low speeds transforms to a dynamic (vibratory) state at elevated speeds. In trials conducted in France and Japan, high speed tracks on flexible ballast foundations have proven to be the safest and most

economical, in contrast to rigid concrete pavements that may cause a sudden change of gradient between slabs, thus elevating the risk of derailment of long carriages. A field trial on the Est-Européenne line, in France, demonstrated that speeds exceeding 400 km/h on ballast beds would be feasible if particle gradations could be optimised to minimise damage to the track. For heavy haul trains (25-30 tonne axle load) in Australia, the effect of critical speeds on the cyclic densification of ballast and associated deformation of the track are significant, in view of stability, safety, and operational efficiency.

Geosynthetics have been widely and successfully used in new rail tracks and in track rehabilitation schemes for almost three decades. When appropriately designed and installed, geosynthetics are a cost effective alternative to more traditional techniques. The applications of geosynthetics within railway construction can be sub-divided into (1) separation, (2) reinforcement, (3) filtration, (4) drainage, (5) moisture barrier/waterproofing and (6) protection. The geocomposites can provide reinforcement to the ballast layer, as well as filtration and separation functions simultaneously. This combination of reinforcement by the geogrid, and the filtration and separation functions provided by the bonded non-woven geotextile, reduce the lateral spreading and fouling of ballast, as well as its degradation, especially in wet conditions. The non-woven geotextile also prevents the fines moving up from the layers of sub-ballast and subgrade (subgrade pumping), thereby keeping the recycled ballast relatively clean. The use of shock mats to mitigate the impact induced ballast degradation is appealing to practitioners. The seepage hydraulics through porous media is influenced by the cyclic loading generated by passing trains. The sub-ballast can act as an effective filter layer that minimises the adverse effects of clay pumping and hydraulic erosion originating from the subgrade. The behaviour of soft clay foundations stabilised with vertical drains and vacuum pressure can now be predicted with acceptable accuracy due to the significant progress made over the past decade through rigorous analytical and numerical analysis.

2 CURRENT DESIGN PRACTICES AND LOGISTICS FOR HIGH SPEED TRAIN

Coal and iron ore comprise almost 80 per cent of the freight carried in Australia. Australia's rail network has the potential to play a much larger role in the mixed passenger and freight operations in metropolitan areas and key inter-city routes. According to a national land freight strategy discussion paper released by Infrastructure Australia in 2010, the total Australian freight movements (combined international and domestic) are expected to double by 2036 and could triple by 2056. While capital cities are likely to accommodate most of population growth, satellite cities, coastal cities, and regional cities will also continue to grow, albeit at different rates. The construction of a proposed high speed train network (length > 1600 km, speed 350 km/h) in Australia is estimated to cost up to $108 billion. This network is expected to carry around 54 million passengers a year by 2036 with competitive fares. The design of a high speed train network faces significant geotechnical challenges due to soft clay deposits in coastal regions, ballast fouling, and track drainage.

Over many years, the design of railway tracks has remained almost unchanged, even though the demand for increased train speed and heavier freight traffic has increased. In Australia, there has been a tendency to concentrate more on the design of track superstructure, while the substructure, consisting of the ballast, sub-ballast, structural-fill and subgrade, is essentially expected to last indefinitely and derives little attention in conventional design methods. The design and selection of appropriate material specifications are serious issues because conventional practices deal with equivalent statics, or at best, the design of road pavements. Several shortcomings, such as quasi-static loading and not cyclic, too uniform particle sizes, while ignoring particle breakage, prevail in the current design practices. This often leads to high track maintenance and interruption of rail services. While an accurate knowledge of the substructure is important in effectively assessing a maintenance plan and associated costs, a significant part of the maintenance budget is allocated to correct track geometry caused by repeated train loading. It is also difficult to understand geotechnical assets, which are characterised by: (i) long design life, (ii) difficult or limited access, (iii) limited flexibility in changing or upgrading the asset, (iv) high replacement/renewal costs, and (v) maintenance that can result in significant operational disruptions, particularly on single lines or those lines where there is no opportunity to re-route services. The heavy haul network (100 MGT annual traffic tonnage) of Queensland Rail (QR) suffers mainly from the breakdown of ballast and intrusion of coal fines. In order to prolong the track maintenance cycle, QR National has recommended the use of uniformly graded ballast, while RailCorp (NSW) has adopted well-graded ballast in their design specifications. Lately, QR National has resorted to the use of sampling and (particularly) trenching to investigate the extent of fouling in planning the track maintenance activities on their four major coal systems (Blackwater, Goonyella, Moura and Newlands). QR National's method of 'capping layer Design' is thus slightly conservative. In addition, wheel-rail irregularities need to be removed promptly in order to avoid additional impact forces, which may lead to failure of the track formation. Finding the means to reduce the maintenance costs and lengthen regular repair cycles has been a priority for most Australian railway organisations occupying one of the busiest traffic schedules in the world.

Apart from being commonly used to protect the ballast layer against subgrade attrition, sub-ballasts are mainly designed to act as a stress dissipation layer (commonly called a capping layer). If ever used as a filtration layer, the design criteria currently used in the industry to select the sub-ballast is still based on the guidelines primarily based on the monotonic

seepage loading common in embankment dams. In rail track environments, the loading system is cyclic and the mechanisms of filtration, interface behaviour, and time dependent changes of the drainage and filtration properties that occur within the filter medium require further understanding. Under the influence of cyclic loading, sub-ballast filtration parameters that are important in conventional rail track design have to be identified and studied in detail.

3 RESEARCH TRENDS IN AUSTRALIA AND ELSEWHERE

Several previous researchers highlighted ballast breakage and confining pressure as the key parameters in the design of ballasted rail tracks (Marshal, 1973; Indraratna *et al*., 2005a; Lackenby *et al.,* 2007). The reorientation and rearrangement of highly angular particles of ballast during such non-uniform triaxial stress conditions primarily contributes to corner (asperities) breakage (Indraratna *et al*., 2005a, 2010a). These broken particles eventually move to the void space in the assembly and cause permanent deformation. Thus breakage and rearrangement of broken particles contributes toward cyclic densification of the assembly (Hossain *et al*., 2007; Lackenby *et al.,* 2007; Indraratna *et al*., 2010a). Under cyclic loads, the cyclic densification of ballast and associated rail track deformations are important for the optimum design, safety and operational efficiency of tracks. The complexities associated with the ballast are attributed to the effects of angularity, anisotropy, particle degradation, and in-situ confining pressure (Raymond and Davies, 1978; Altuhafi and Coop, 2011) as well as the frequency of applied load cycles (Luo *et al.,* 1996; Indraratna *et al*., 2010b).

According to literature, very limited studies have been conducted on the adverse effects of coal fouling on the strength of ballast have been conducted (Han and Selig, 1997; Budiono *et al*., 2004; Tutumluer *et al*., 2008; Dombrow *et al.,* 2009). When ballast is fouled by breakage or infiltration of fine particles, the interaction between particles may change considerably as fine particles clog the ballast voids and grid apertures, reducing the interlocking and frictional resistance between the geogrid and ballast. Fine particles adversely affect the strength and stiffness of track structures (Indraratna *et al*., 2011c; Budiono *et al*., 2004) because as fouling increases, the stiffness of the ballast is significantly reduced. When the amount of fouling materials is excessive, fine particles can dominate the ballast behaviour and ultimately make the track unstable. The sub-ballast dissipates the stress transferred from the overlying layer of ballast and acts as a filter layer that minimises the adverse effects of clay pumping and hydraulic erosion. In spite of the importance of its role, little research has been conducted on sub-ballast as a filtration layer. Locke *et al*. (2001) highlighted that an evaluation of the effectiveness of filters based on the constriction size distribution (CSD) can be more appropriate than the sole use of particle sizes. The development and effectiveness of constriction based retention criteria, valid for both uniform and well graded materials based on experimental evidence, were presented (Trani and Indraratna, 2010a,b).

It is expected that the use of geosynthetics will encourage the re-use of discarded ballast from stockpiles, reducing the need for further quarrying and getting rid of the unsightly spoil tips often occupying valuable land in metropolitan areas. The potential use of geosynthetics to improve track stability has been observed in several laboratory studies (Selig and Waters, 1994; Rowe and Jones, 2000; Raymond, 2002; Indraratna and Salim, 2003; Indraratna *et al*., 2010a). However, only a few studies have assessed the relative merits of geosynthetics and shock mats under *in situ* track conditions, while the 'field' performance of different types of geosynthetics to improve the overall stability of ballasted rail tracks has not been investigated in a systematic manner. Two extensive field studies were carried out to fill this gap. This paper discusses the details of field instrumentation and monitoring processes along with the preliminary findings of these unique studies.

Many coastal regions of Australia contain very soft clays (estuarine or marine), which have undesirable geotechnical properties such as low bearing capacity and high compressibility. In the absence of appropriate ground improvement (Indraratna and Redana, 1998; Bergado *et al*., 2002; Indraratna *et al.,* 2009), excessive settlement and lateral movement often prevent the construction of buildings, and port and transport infrastructure, including highway and rail embankments built on such soft ground (Holtz *et al.,* 1991; Indraratna and Redana, 2000). When railways are constructed on poorly drained soft formations, the increase in pore pressures due to the undrained cyclic load behaviour will decrease the effective load bearing capacity of the formation. Even if the rail tracks are well built structurally, undrained formation failures can adversely influence train speeds, apart from the inevitable operational delays. Under circumstances of high excess pore water pressures, clay slurrying may initiate pumping the slurried soil upwards under cyclic loads, clogging the clean ballast and causing poor drainage (Indraratna and Salim, 2005). This can cause poor track geometry and imperfections, track instability and the need for speed restrictions. Through the Sandgate case study, the design methodology and finite element analysis of a rail track stabilised with relatively short prefabricated vertical drains (PVDs) are presented. It was shown that these relatively short PVDs, between 6 m to 8 m in length, could still be enough to dissipate train induced pore pressures, limit lateral movements and increase the shear strength and bearing capacity of the soft formation.

4 EXTENDING THE CURRENT STATE OF THE ART

4.1 SHEAR STRENGTH

The shear strength of granular materials is generally assumed to vary linearly with applied stress, and the Mohr-Coulomb theory is conveniently used to describe its conventional shear behaviour. The shear strength of ballast is a function of confining pressure, and is highly non-linear at high stresses (Indraratna et al., 1997, 2000; Ramamurthy, 2001). Indraratna et al. (1993) proposed a non-linear strength envelope obtained while testing granular media at low normal stresses. This non-linear shear stress envelope is represented by the following equation:

$$\tau_f / \sigma_c = m\,(\sigma'_n / \sigma_c)^n \qquad (1)$$

where τ_f is the shear stress at failure, σ_c is the uniaxial compressive stress of the parent rock determined from the point load test, m and n are dimensionless constants, and σ'_n is the effective normal stress. The non-linearity of the stress envelope is governed by the coefficient n.

For the usual range of confining pressures (below 200 kPa) for rail tracks, n takes values in the order of 0.65 - 0.75. A large-scale cylindrical triaxial apparatus, which could accommodate specimens 300 mm diameter and 600 mm high (Figure 1), was used by Indraratna *et al*. (1998) to verify the non-linearity of shear stress. The results of his study associated with latite basalt in a normalised form are plotted in Figure 2, with results obtained from other researchers [Marachi *et al*., 1972; Marsal, 1973; Charles and Watts, 1980].

Figure 1: Cylindrical triaxial apparatus equipped with a dynamic actuator at University of Wollongong

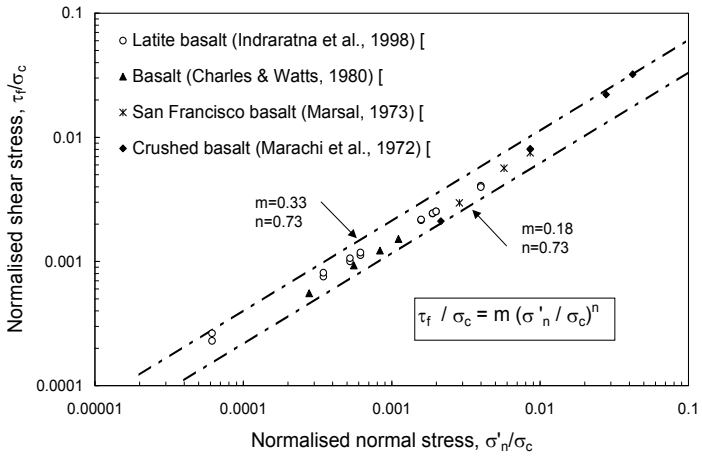

Figure 2: Normalised shear strength for latite basalt aggregates (after Indraratna *et al*., 1998)

4.2 BALLAST BREAKAGE

Railway tracks are severely affected by the degradation of ballast particles (Indraratna *et al*., 2011a,d,e). Their breakage under load is a complex mechanism that usually starts at the inter-particle contacts (i.e. breakage of asperities), followed by a complete crushing of weaker particles under further loading. A rapid fragmentation of particles and subsequent clogging of voids with fines is commonly observed in rail track foundations. The degradation of aggregate is the primary cause of contamination, and accounts for up to 40% of the fouled material (Chrismer and Read, 1994). The main factors that generally affect breakage can be divided into three categories: (a) properties related to the characteristics of the parent rock (e.g. hardness, specific gravity, toughness, weathering, mineralogical composition, internal bonding and grain texture); (b) physical properties associated with individual particles (e.g. soundness, durability, particle shape, size, angularity and surface smoothness) and (c) factors related to the assembly of particles and loading conditions (e.g. confining pressure, initial density or porosity, thickness of the ballast layer, ballast gradation, the presence of water or the moisture content of the ballast, repeated loading pattern including load amplitude and frequency). The effects of some of these factors are demonstrated in this paper.

Indraratna *et al.* (2005a) introduced a new Ballast Breakage Index (BBI) specifically for railway ballast to quantify the extent of degradation, and it is based on the particle size distribution (PSD) curves. The ballast breakage index (BBI) is calculated on the basis of changes in the fraction passing a range of sieves, as shown in Figure 3. The increase in degree of breakage causes the PSD curve to shift further towards the region of smaller size particles on a conventional PSD plot. The area A between the initial and final PSD increases, results in a greater BBI value. BBI has a lower limit of 0 (no breakage) and an upper limit of 1. By referring to the linear particle size axis, BBI can be calculated using the following equation.

$$BBI = \frac{A}{A+B} \quad \textbf{(2)}$$

where A is the area defined previously, and B is the potential breakage or area between the arbitrary boundary of maximum breakage and the final particle size distribution.

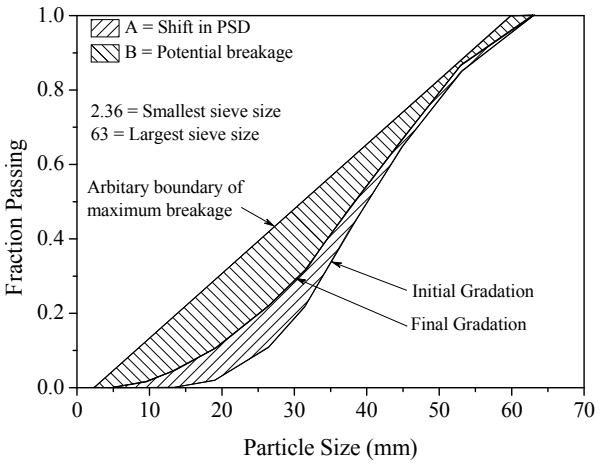

Figure 3: Ballast breakage index (BBI) calculation method (data sourced from Indraratna *et al*., 2005a)

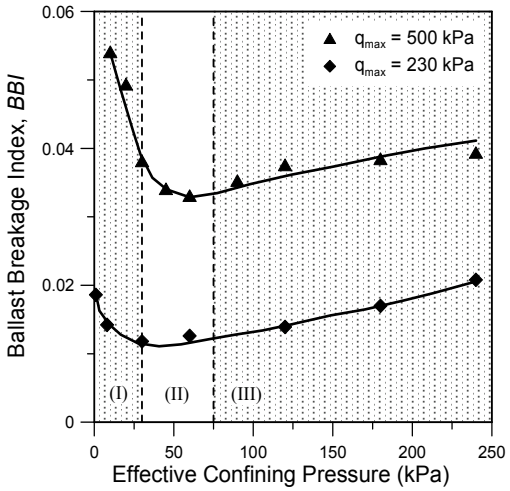

Figure 4: Effect of confining pressure on particle degradation (data sourced from Lackenby *et al.,* 2007)

4.4 CONFINING PRESSURE

Track substructure is essentially self supporting with minimal lateral constraints. Although the effect of confining pressure on various geotechnical structures is significant and is considered to be key criteria in the design of these structures, it is usually neglected in conventional rail track design. During the passage of a train, the ballast and sub-ballast materials are free to spread laterally, which decreases its shear strength, while increasing track settlement. A series of cyclic triaxial tests were conducted on samples of ballast to investigate the effect of confining pressure on ballast under cyclic loading, to reduce the volume of breakage and find out the optimum confining pressure based on loading and track conditions.

Specimens were prepared to the recommended gradation and initial porosity (i.e. d_{50} = 38.5 mm, C_u = 1.54, e_o = 0.76 where d_{50} is the diameter of the ballast corresponding to 50% finer in the particle size distribution curve, and C_u is the coefficient of uniformity). Effective confining pressures (σ_3') ranging from 1 to 240 kPa with q_{max} = 500 kPa were applied. Lackenby *et al*. (2007) proposed that the degradation of ballast under cyclic loading can be categorised into three distinct zones, namely: (I) the Dilatant Unstable Degradation Zone (DUDZ), (II) the Optimum Degradation Zone (ODZ) and (III) the Compressive Stable Degradation Zone (CSDZ), as shown in Figure 4. These zones are defined by the magnitude of confining pressure (σ_3') applied to the specimen (i.e. DUDZ: $\sigma_3' < 30$ kPa, ODZ: 30 kPa $< \sigma_3' <$ 75 kPa, CSDZ: $\sigma_3' > 75$ kPa). However, the maximum deviator stress magnitude ($q_{max,cyc} = \sigma_1'_{max} - \sigma_3'$) and maximum static peak deviator stress ($q_{peak,sta}$) also plays an important role in characterising these degradation zones (Lackenby *et al*. 2007). Track confinement can be increased by reducing the spacing of sleepers, increasing the height of the shoulder ballast, including a geosynthetic layer at the ballast-subballast interface, widening the sleepers at both ends and using intermittent lateral restraints at various parts of the track (Indraratna *et al*., 2004).

4.4 INFLUENCE OF TRAIN SPEED (FREQUENCY)

In this investigation the influence of frequency on the deformation and degradation of ballast during cyclic loading was studied using the large scale cyclic triaxial equipment designed and built at the University of Wollongong (Indraratna *et al.*, 2010b). The dynamic stresses imparted to the ballast that correspond to different frequencies were estimated in accordance with Esveld (2001). Latite ballast was thoroughly cleaned, dried, and sieved through a set of sieves (53 mm,

45 mm, 37.5 mm, 31.5mm, 26.5 mm and, 19 mm). Ballast specimens were placed inside a 5 mm thick Neoprene rubber membrane in four separate layers to a density of 1530 kg/m^3. These specimens were then isotropically consolidated to a confining pressure of 60 kPa. Cyclic tests up to 100,000 cycles were conducted at frequencies of 10 Hz, 20 Hz, 30 Hz, and 40 Hz. Numerical model was developed in PFC^{2D} to apply a stress controlled cyclic biaxial test at the desired frequency (f) and amplitude of cyclic loading. Sub-routines were developed to represent irregular ballast particles.

Figure 5 presents the variation of axial strain (ε_a) with the number of cycles (N) for different frequencies (f) of loading. A significant increase in ε_a with f can be observed. For a particular value of f, ε_a rapidly increases to maximum value (e.g. 6.1 % at N = 2,500 for f =10 Hz) in the initial cycles, after which a permanent ε_a attains a stable value at large N. This sudden increase in ε_a at low values of N can be attributed to the particle re-arrangement and corner breakage. In addition, it is evident that with an increase in f, higher values of N are required to stabilise ε_a.

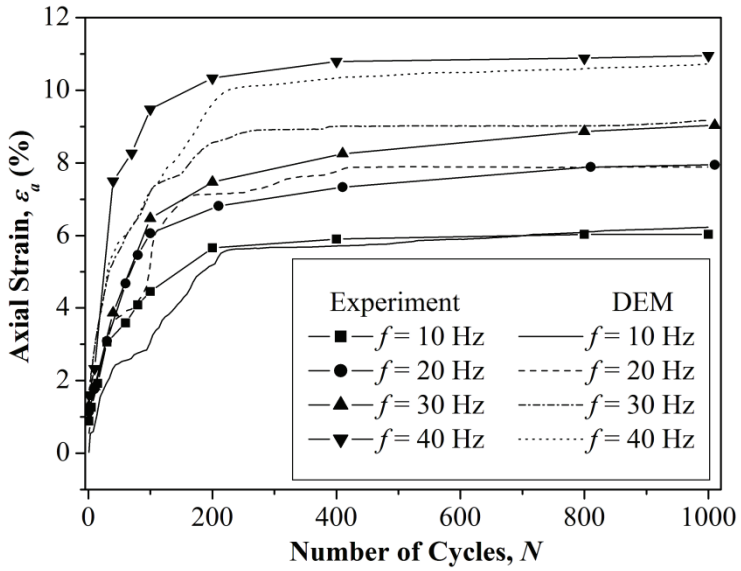

Figure 5: Comparison of axial strain (ε_a) predicted by DEM with experiment results (Indraratna *et al*., 2010b)

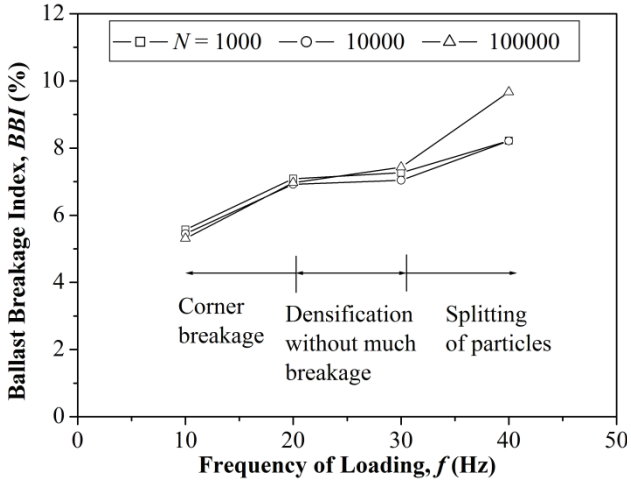

Figure 6: Variation of ballast breakage index (BBI) with various frequencies (f) (Indraratna *et al*., 2010b)

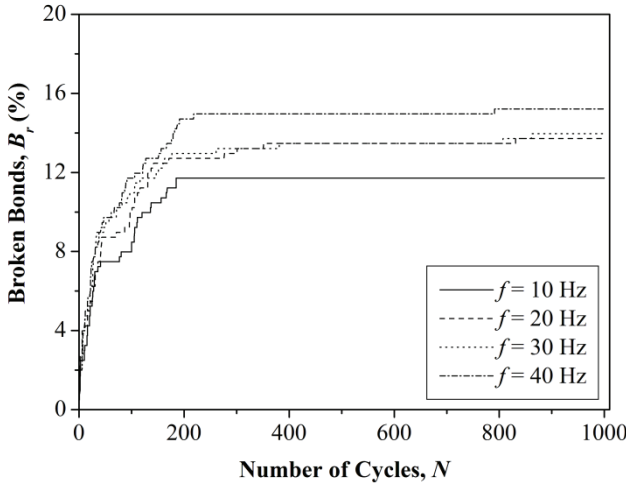

Figure 7: Effects of frequency (f) on bond breakage (Br) with number of cycles (N) (Indraratna *et al.,* 2010b)

The influence of f and N on ballast breakage is presented in Figure 6. Ballast breakage has been quantified in terms of BBI for different values of f and N. The BBI is found to increase with f, but at lower values of f (e.g. $f \leq$30 Hz) BBI is not influenced by N. This clearly highlights that most ballast breakage takes place within 1000 cycles. A significant increase in BBI can be observed in the range 10 Hz $\leq f \leq$ 20 Hz, a marginal increase in BBI in the zone 20 Hz $< f \leq$ 30 Hz, and a rapid increase in BBI as $f >$ 30 Hz. It has been observed from the laboratory tests that in the zone 10 Hz $\leq f \leq$ 30 Hz, corner breakage is more pronounced, while considerable splitting of ballast particles across their bodies can be observed at $f >$ 30 Hz. In the range 20 Hz $\leq f \leq$ 30 Hz, the ballast becomes denser under cyclic loading without much

additional breakage. However, more pronounced breakage occurs as $f > 30$ Hz. High permanent deformation observed at higher frequencies can be attributed to an increase in particle degradation. Figure 7 shows the cumulative bond breakage (B_r), defined as a percentage of bonds broken compared to the total number of bonds at different f and N. It can be observed that B_r increases with increase in f and N. Most of the bond breakages occurred during the initial cycles of loading, causing higher permanent ε_a. Once the bond breakage ceases, there is an insignificant increase in ε_a. This clearly highlights that particle degradation is one of the major sources responsible for permanent deformation.

4.5 BALLAST FOULING

Ballast is a free draining material with sizes ranging from 10 mm to 63 mm and contains large void spaces. However, the infiltration of fouling material reduces the void and restricts track drainage. The crushed rock fines (due to particle breakage), coal fines (due to spillage from coal wagons) and clay-silt fines (due to pumping of soft saturated subgrade) accumulate within the voids (i.e. fouling) of the ballast bed and impair track drainage. Ballast fouling due to coal and subgrade fines, and the subsequent formation of mud holes in the Goonyella System, QR National, is shown in Figures 8 and 9. Several fouling indices are used in practice to measure fouling. Selig and Waters (1994) have defined the fouling index as a summation of percentage (by weight) passing the 4.75 mm sieve and 0.075 mm sieve. They also proposed a percentage of fouling which is the ratio of the dry weight of fouled material passing through a 9.5 mm sieve to the dry weight of the total fouled ballast sample. These mass based indices give a false measurement of fouling when the fouling material has a different specific gravity. Therefore, Feldman and Nissen (2002) defined the Percentage Void Contamination (PVC) as the ratio of bulk volume of fouling material to the volume of voids of ballast when it is clean. However, this PVC method does not consider the effect of the void ratio, gradation and specific gravity of the fouling material, which is the main factor affecting ballast drainage. Therefore, a new parameter Void Contaminant Index (VCI) is proposed to incorporate effects of void ratio, specific gravity and gradation of fouling material and ballast (Indraratna *et al.,* 2010c):

$$VCI = \frac{(1+e_f)}{e_b} \times \frac{G_{sb}}{G_{sf}} \times \frac{M_f}{M_b} \times 100 \quad \textbf{(3)}$$

where e_b is the void ratio of clean ballast, e_f is the void ratio of fouling material, G_{sb} is the specific gravity of the ballast material, G_{sf} is the specific gravity of the fouling material, M_b is the dry mass of clean ballast, and M_f is the dry mass of the fouling material.

Figure 8: Mudholes caused by excessive coal/clay fouling (Goonyella System, QR National: Photo courtesy of Michael Martin)

Figure 9: Ballast fouling due to coal and subgrade pumping (Goonyella System, QR National: Photo courtesy of Michael Martin)

In general, ballast specifications in Australia and around the world demand a uniform gradation (uniformity coefficient, C_u = 1.5 - 3.0) to fulfil the requirements for rapid track drainage. Also, the void ratio of clean ballast (e_b) will not change significantly. However, there is a significant variation in the void ratio (e_f), specific gravity (G_{sf}), and gradation characteristics of fouling material such as sand, silt, clay, coal and crushed rock fragments and the VCI can take all these variations into account. To study the effects of fouling, a series of large scale constant head permeability tests (AS 1289.6.7.3, 1999) on fouled ballast with different percentages of coal, clayey sand and kaolin were conducted. The large scale permeability test chamber ,which could accommodate specimens 500 mm in diameter and 500 mm high was used in this study (Figure 10). The fouled specimen was saturated for at least 24 hours before testing. A constant head was ensured with a steady state flow subjected to a 1.5 m head of water by an adjustable overhead tank. The bulk unit weights of clean ballast, coal, clayey sand and kaolin clay were 15.98, 8.5, 12.5, and 8.9 kN/m^3, respectively. The specific gravities of clean ballast (G_{sb}) and fouling materials (G_{sf}) namely: coal, clayey sand and kaolin clay were 2.75, 1.5, 2.6, and 2.51 respectively.

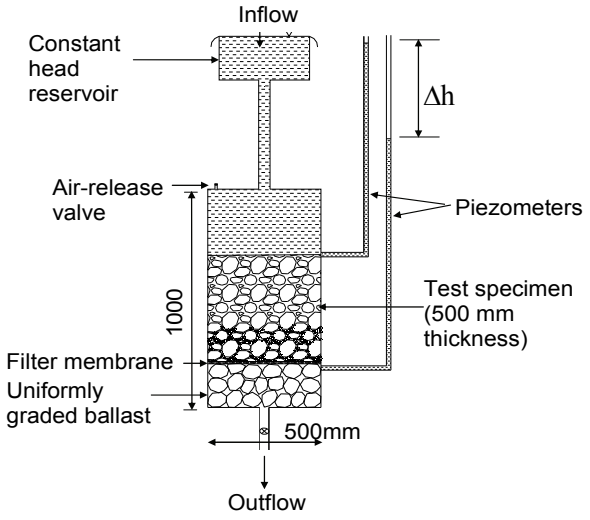

Figure 10: Schematic diagram of large scale permeability test apparatus (data sourced from Tennakoon *et al*., 2012)

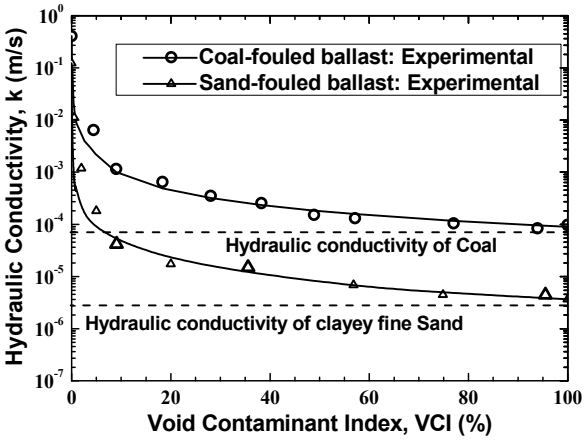

Figure 11: Variation of the hydraulic conductivity with VCI (data sourced from Tennakoon *et al*., 2012)

Figure 11 shows the variations of hydraulic conductivity of coal fouled and sand fouled ballast with VCI where the fouling material was distributed non-uniformly. As expected, the overall hydraulic conductivity of fouled ballast always decreased with an increase in VCI. The current test results showed that a 5% increase in the VCI decreased the hydraulic conductivity by a factor of at least 200 and 1500 for ballast contaminated by coal and clayey sand, respectively. However, this reduction in permeability would not significantly affect the minimum drainage capacity needed for acceptable track operations. Beyond a VCI of 75%, any further reduction in hydraulic conductivity became marginal because it approached the hydraulic conductivity of the fouling material itself. Figure 12 presents a track maintenance chart based on seepage analysis using SEEP/W software (Tennakoon *et al.,* 2012). When the top layer of ballast is clean, the track can be classified either as 'free drainage' or as 'acceptable drainage'. If the top layer has a VCI >50% lying on a relatively clean layer of bottom ballast then the drainage capacity can be considered as 'poor'. When all layers have a VCI >50%, then the track is considered to be 'very poor drainage' and therefore requires maintenance. This analysis clearly suggests that replacing or cleaning the ballast from the shoulder is more than adequate, when the top layer has a VCI that is less than 50%. But when the VCI of shoulder ballast exceeds 50%, it acts as a flow barrier and the drainage capacity of the track decreases significantly, and is categorised as 'poor drainage'. Moreover, cleaning the shoulder ballast alone is not effective if the top layer of ballast is badly fouled (> 50 %).

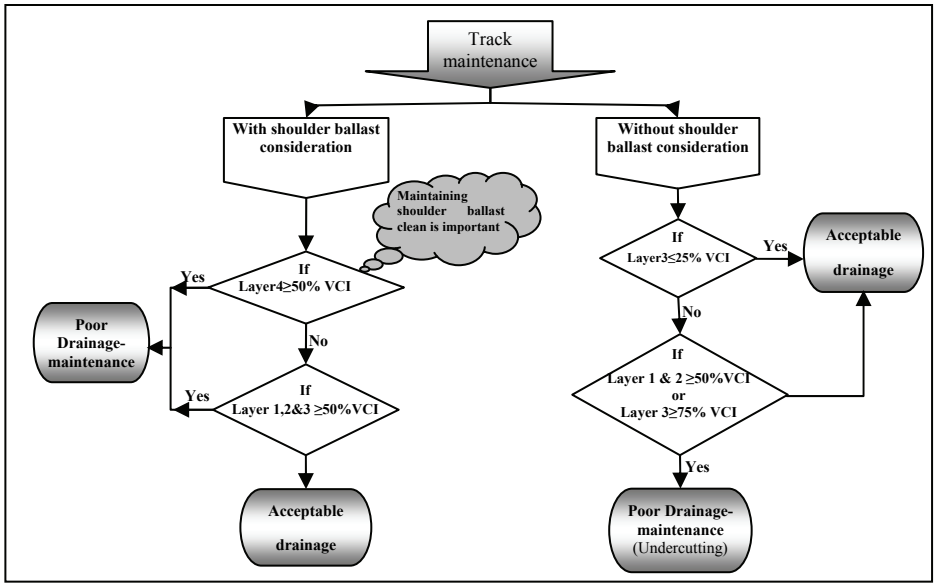

Figure 12: Maintenance chart (data sourced from Tennakoon *et al*., 2012)

4.6 USE OF GEOGRID FOR STABILISING FOULED BALLASTED TRACK

The shear strength and apparent angle of the shearing resistance of clean ballast and coal fouled ballast was evaluated under various degrees of fouling using the large scale direct shear apparatus described in this section. The recommended particle size distribution of ballast (mean particle size (d_{50}) = 35 mm) was adopted. Using a parallel gradation, the maximum size of the ballast tested in the laboratory was less than 40 mm, which was small enough to avoid any boundary effects. Coal fines were used as fouling material. A polypropylene geogrid with 40 x 40 mm^2 aperture was used. The direct shear test apparatus consisted of a 300 x 300 mm^2 square steel box 195 mm high that was divided horizontally into two equal halves. A schematic diagram of the test set up is shown in Figure 13. The clean ballast aggregates were compacted in the bottom half of the shear box to a dry density of 15 kN/m^3 and then a sheet of geogrid was placed on top. The remaining ballast was then compacted in the upper half of the shear box. Coal fines were spread over each compacted layer of ballast in accordance with the desired VCI.

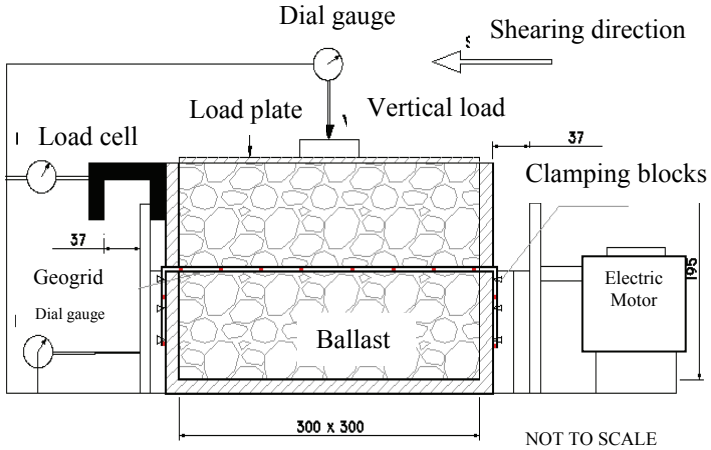

Figure 13: Schematic diagram of the large-scale direct shear test set up (Indraratna *et al.,* 2011c)

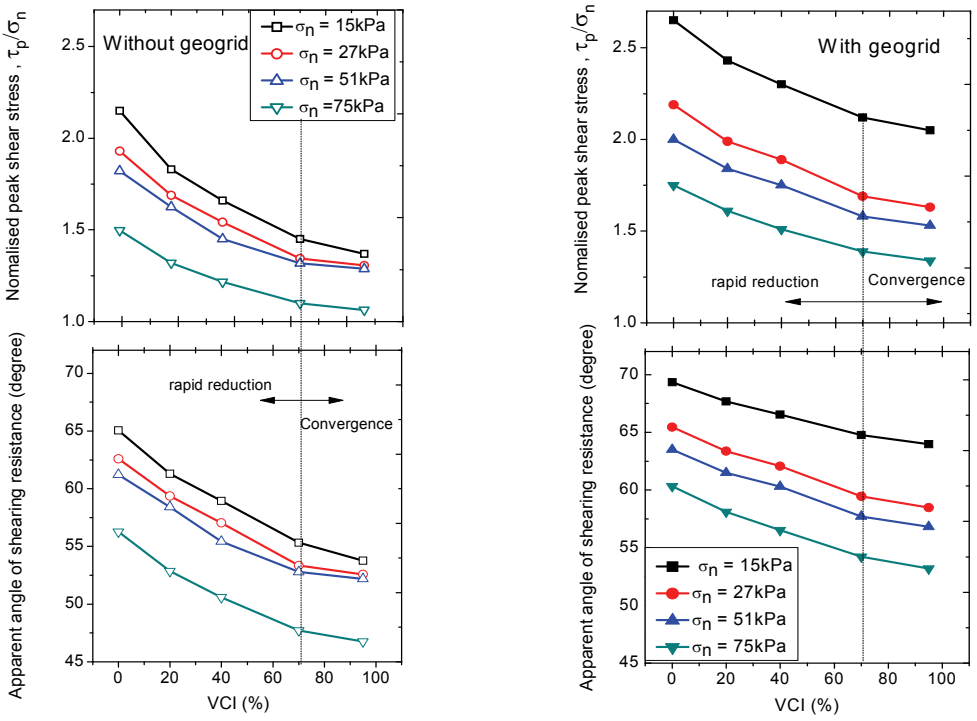

(a) (b)

Figure 14: Effect of VCI on normalised peak shear strength and apparent angle of shearing resistance of ballast: (a) without geogrid and (b) with geogrid (Indraratna *et al.,* 2011c, Copyright (2012), with permission from Elsevier)

The tests were conducted at four normal stresses of 15, 27, 51, and 75 kPa. The lower section of the shear box was moved at 2.5 mm/min, while the upper section of the box remained stationary. Each specimen was subjected to 37 mm of maximum horizontal displacement. The normalised peak shear stress (τ_p/σ_n) and apparent angle of shearing resistance (ϕ) of clean ballast and coal-fouled ballast are plotted for different values of VCI (Figure 14). It is evident that the increase in shear stress per unit of normal stress was non-linearly proportional to the normal stress and increased slightly when the normal stress increased.

The coal fines steadily reduced the peak shear stress of the coal-fouled ballast due to a reduction in the apparent angle of shearing resistance. This decrease in the shear strength of unreinforced and reinforced coal-fouled ballast is significant when the VCI increased up to 70%, beyond which any further reduction in the shear strength becomes marginal. The apparent friction angle of clean ballast varied between 48^0 and 65^0, depending on the applied normal stress.

4.7 EFFECT OF THE GEOGRID APERTURE SIZE ON THE INTERFACE SHEAR STRENGTH

In order to investigate the role played by the size of the geogrid aperture on the strength of the ballast-geogrid interface for different types of geogrids, a series of large-scale direct shear tests were conducted. Fresh latite basalt with recommended gradations (D_{50} = 35 mm) and seven geogrids with different aperture sizes (A) were used for this study. Their physical characteristics and technical specifications are given elsewhere (Indraratna *et al*., 2011b). Geogrid was placed at the interface of the upper and lower sections of the shear box assembly with the machine direction placed parallel to the direction of shearing. Tests were conducted at normal pressures of 26.3, 38.5, 52.5, and 61.0 kPa, using a shear rate of 2.75 mm/min. All the tests were conducted to a maximum shear displacement of 36 mm. The behaviour of the ballast-geogrid interface could be examined on the basis of the interface efficiency factor (α), which is defined as the ratio of the shear strength of the interface to the internal shear strength of the soil. Figure 15 shows the variation of α with A/D_{50} ratio. It was observed that α increased with A/D_{50} until it attained a maximum value of 1.16 at A/D_{50} of 1.21, and then it decreased towards unity as A/D_{50} approached 2.5. The value of $\alpha < 1$ indicated that the particles were not interlocked, whereas when $\alpha > 1$ they were, which effectively increased the shear strength. Based on this variation of α, the ratio A/D_{50} was then classified into three primary zones, as explained below:

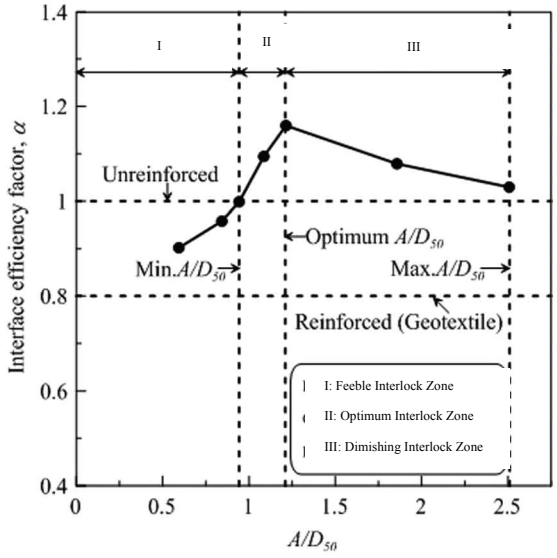

Figure 15: Variation of interface efficient factor (α) with A/D_{50} ratio (Indraratna *et al.,* 2011b, Reprinted with permission from ASTM Geotechnical Testing Journal, copyright ASTM International, 100 Barr Harbor Drive, West Conshohocken, PA 19428)

4.7.1 Feeble interlock zone ($0.95 > A/D_{50} > 0$)

In this zone the particle-grid interlock was weaker than the inter-particle interaction achieved without geogrid because the particle-grid interlock was only attributed to smaller particles ($<0.95D_{50}$) compared to the particle-particle interlock with respect to all sizes. An examination after testing showed insignificant particle breakage, which suggests the interface failure originated from a loss of particle-grid interlock during shearing.

4.7.2 Optimum interlock zone ($1.20>A/D_{50}>0.95$)

In this zone the interlocking of relatively larger particles occurred, which lead to the values of α exceeding unity. The value of α attained a maximum of 1.16 at an optimum A/D_{50} ratio of about 1.20. An examination after shearing showed there were many broken particles at the interface, suggesting that the failure was caused by the breakage of initially interlocked particles.

4.7.3 Diminishing interlock zone ($A/D_{50}>1.20$)

In this zone the values of α were greater than unity but the degree of interlocking decreased rapidly, leading to a reduction in α with an increasing A/D_{50} ratio. It was observed that α decreased to almost unity when A/D_{50} exceeded 2.50. This implies that the interface responds in a similar manner as unreinforced ballast; as the apertures increase in size in relation to the sizes of the ballast particles.

The minimum and maximum size apertures of geogrid required to achieve maximum efficiency was $0.95D_{50}$ and $2.50D_{50}$ respectively. For all practical purposes, the optimum size aperture of geogrid can be $1.15\text{-}1.3D_{50}$.

4.8 USE OF SHOCK MATS FOR MITIGATING BALLAST BREAKAGE INDUCED BY IMPACT

In this study a series of laboratory tests were carried out to evaluate the effectiveness of shock mats in the attenuation of high frequency impact loads and subsequent mitigation of ballast deformations and degradation. Large scale drop-weight impact testing equipment was used for this study. Latite is commonly used as railway ballast in NSW, Australia and its physical and other index properties are discussed elsewhere (Indraratna *et al.,* 1998). The particle size distribution of ballast specimens was prepared in accordance with the current practice in Australia [AS 2758.7, 1996]. A thin layer of compacted sand was used in the laboratory physical model to simulate a typical 'weak' subgrade. The 10 mm thick shock mat used in the study was made of recycled rubber granulates of 1-3 mm size particles, bound by polyurethane elastomer compound (tensile strength = 600 kN/m^2, tensile strain at failure = 80%, Modulus at 10% compressive strain = 3800 kN/m^2). In order to resemble low track confining pressure in the field, the test specimens were confined in a rubber membrane thick enough to prevent piercing by sharp particles during testing (Figure 16a). A steel plate (D = 300 mm, t = 50 mm) was used to represent a hard base such as the deck of a bridge, or rock structure etc., where breakage from impact loads becomes pronounced in the field. In order to simulate relatively weak subgrade conditions, a 100 mm thick, vibro-compacted sand cushion was placed below the ballast bed. Three layers of shock mat with a combined thickness of 30 mm were used. The drop hammer was raised mechanically to the required height and then released by an electronic quick release system. The impact load was stopped after 10 blows due to an attenuation of strains in the ballast layer.

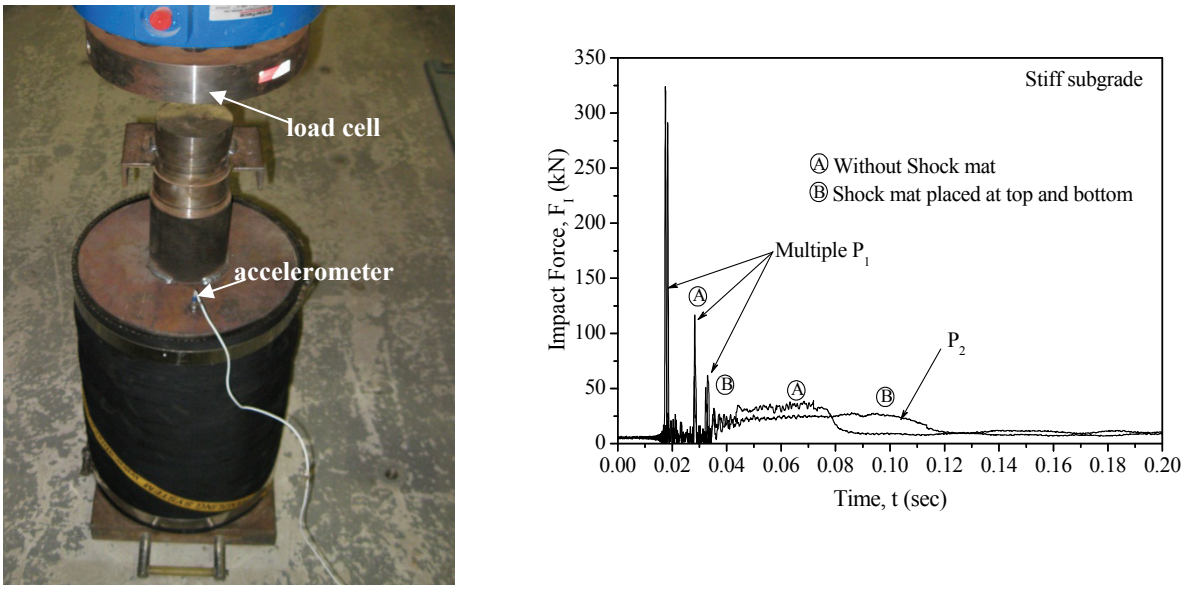

(a) (b)

Figure 16: (a) Test Sample; (b) Typical impact force responses for stiff subgrade (data sourced from Nimbalkar *et al*., 2012).

The impact load-time history under a single impact load (1st drop of the free fall hammer) is shown in Figure 16b. Two distinct types of peak forces were seen during impact loading, an instantaneous sharp peak with very high frequency, and a gradual peak of smaller magnitude with relatively lesser frequency. Jenkins *et al.* (1974) termed these peak forces

as P_1 and P_2 respectively, which is now universal terminology widely used by track engineers. It was also evident that multiple P_1 type peaks followed by the distinct P_2 type peak often occurred. The multiple P_1 peaks occurred when the drop hammer was not restrained vertically, so that it rebounded after the first impact and hit the specimen again. The observed benefits of a shock mat are therefore twofold: (a) it attenuates the impact force and (b) it reduces the impulse frequencies thereby extending the time duration of impact. After each test the ballast sample was sieved and a change in gradation was obtained. Breakage was quantified using Ballast Breakage Index (BBI), proposed by Indraratna *et al.* (2005a). The BBI values are presented in Table 1.

Table 1: Ballast breakage under impact loading (Indraratna *et al.,* 2011b).

Test No.	Base type	Shock Mat Details	*BBI*
1	Stiff	Without shock mat	0.170
2	Stiff	Shock mat at top and bottom of ballast	0.091
3	Weak	Without shock mat	0.080
4	Weak	Shock mat at top and bottom of ballast	0.028

The higher breakage of ballast particles can be attributed to the considerable non-uniform stress concentrations occurring at the corners of the sharp angular particles of fresh ballast under high impact induced contact stresses. The impact from just 10 blows caused considerable breakage (i.e. BBI = 17%) when a stiff subgrade was used, but when a shock mat was placed above and below the ballast bed, particle breakage was reduced by approximately 47% for a stiff subgrade and approximately 65% for a weak subgrade. The weak subgrade itself acts as a flexible cushion.

4.9 THE BEHAVIOUR OF THE SUB-BALLAST (FILTER) UNDER CYCLIC TRAIN LOADING

In rail track environments, the loading system is cyclic unlike the monotonic seepage force that usually occurs in embankment dams. The mechanisms of filtration, interface behaviour, and time dependent changes of the drainage and filtration properties occurring within the filter medium require further research to improve the design guidelines. To simulate the dynamic train loading conditions applied on a granular filter medium, a cyclic loading filtration apparatus was designed at the University of Wollongong. A standard testing procedure was established to monitor the performance of a granular filter which was previously identified as satisfactory based on existing available filtration criteria.

4.9.1 Experimental Methodology

To simulate dynamic train loading conditions applied on a granular filter medium, a cyclic loading filtration apparatus was designed. The test apparatus consists of a chromium plated cylinder with an inside diameter of 240 mm, a wall thickness of 5 mm and a height of 300 mm.

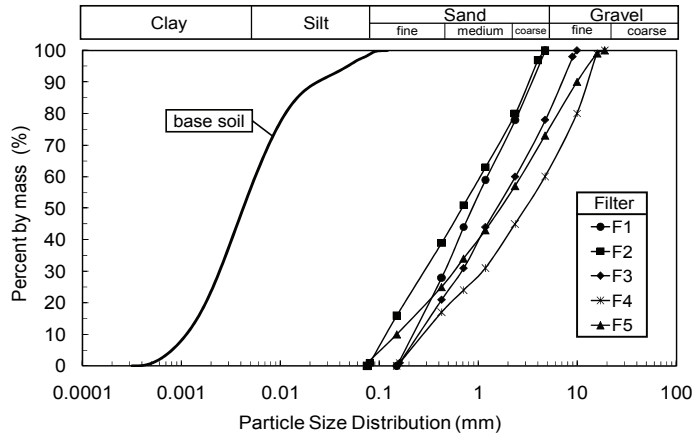

Figure 17: The particle size distribution of the filters and base soil (Trani and Indraratna, 2010a)

To simulate the filtration action in the event of clay pumping occurring in rail track environments, clay or silt slurry is pumped from the bottom of the setup while a cyclic load is applied from the top. A detailed soil specific calibration procedure is discussed by Trani and Indraratna (2010c). Through these probes, real time changes in the porosity of the filter are measured. Crushed basaltic rock road base material which is naturally well graded and has a uniformity coefficient (C_u) of 17 is used as a granular filter sub-ballast. The angular road base material is carefully sieved into a range of particle sizes, washed, oven dried and remixed into a predetermined particle size distribution (PSD). The PSD of the filters *F1* to *F5* is shown in Figure 17. The base soil is a low plasticity and highly dispersive and erodible silty

clay. In simulating a heavy haul train, a uniform cyclic stress in the form of a simple harmonic function is applied in an increasing frequency of 5, 10, 15, 20 and 25 Hz. Using a two dimensional stress distribution for a plane strain scenario, the train load is replicated in the modified permeameter using the dynamic actuator with a set of cyclic stresses applied to a minimum of 100,000 cycles. The specimen was subjected to a uniform minimum stress of 30 kPa and maximum stress of 70 kPa.

4.9.2 Test Results and Analysis

As shown in Figure 18a, rapid compression for all types of sub-ballast occurred during the first 7,500 cycles, irrespective of its grading or the range of particle sizes of which it is composed. The introduction of base soil during the slurry tests does not alter the strain development of the filter (Figure 18b). Moreover, each type attains a stable configuration at about 20,000 cycles. The compressive behaviour allows the voids spaces of the filter medium skeleton to close up and hence, reduce the porosity. The amount of fines coming from the degradation of filter grains with time, which has a potential to become part of the filter skeleton or may fill the voids, is of an insignificant level. The average mass percentage of fines less than or equal to 150 μm produced after the test is less than 5%. This is best explained by the existence of optimum internal contact stress distribution and increased inter-particle contact areas.

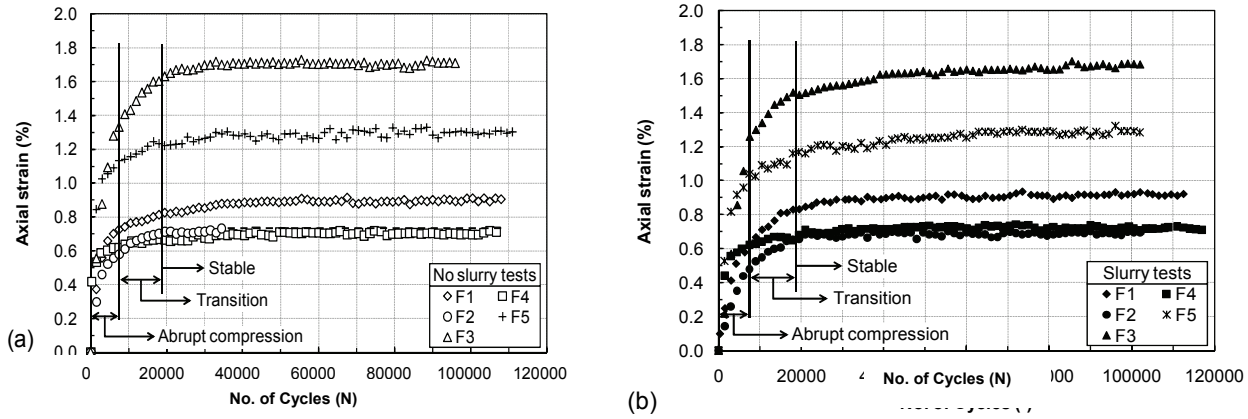

Figure 18: Development of strain under cyclic loading for all filter types during (a) no slurry test, and (b) slurry tests (Trani and Indraratna, 2010b).

4.10 USE OF GEOSYNTHETIC VERTICAL DRAINS AS SUB-SURFACE DRAINAGE

Low lying areas with large volumes of plastic clays can sustain high excess pore water pressures during static and repeated loading. In low permeability soils, the increase in excess pore pressures has an adverse effect on the effective load bearing capacity of the soil formation. Under certain circumstances, clay pumping beneath rail tracks may pump the soil upwards and foul the ballast bed and promote undrained shear failure (Chang, 1982; Indraratna *et al.*, 1992). Geosynthetic prefabricated vertical drains (PVDs) can be used to dissipate excess pore pressures by radial consolidation before they can develop to critical levels. These PVDs continue to dissipate excess pore water pressures even after the cyclic load ceases (Indraratna *et al*., 2009a).

4.10.1 Apparatus and test procedure

The tests were conducted using the large scale process simulation triaxial equipment. This equipment was modified to measure the excess pore water pressure at various locations inside the specimen. Six miniature pore pressure transducers were installed through the base of the triaxial rig and then inserted into the base of the specimen and in the positions shown in Figure 19a. The clay was kaolinite with a specific gravity G_s 2.7. The liquid limit w_L was 55% and the plastic limit w_P was 27%. The compression index c_c was 0.42 and the swelling index c_s was 0.06. The soil specimens (with and without PVD) were prepared under anisotropic consolidation with an effective vertical stress of 40 kPa ($K_0 = 0.60$ representing the *in situ* stress), where K_o is the ratio of the effective horizontal to the effective vertical stress. Dual drainage through the top and bottom of the specimen was permitted to attain a 95% degree of consolidation at 5 weeks with PVD, and 9 weeks without PVD. Three different series of tests were conducted: (a) cyclic partially drained with PVD, (b) cyclic consolidated undrained (cyclic CK_oU) without PVD and (c) cyclic unconsolidated undrained (cyclic UU) without PVD. A series of conventional monotonic triaxial tests were first carried out according to ASTM (2002) to determine the maximum deviator stress at failure (q_f). Then a cyclic stress ratio (CSR) of 0.65 was chosen, where CSR is defined as the ratio of the cyclic deviator stress q_{cyc} to the static deviator stress at failure q_f. The

term critical cyclic stress ratio is defined as the level of cyclic deviator stress above which a sample would experience failure after a certain number of loading cycles.

Failure is a condition of rapidly non-recoverable deformation with an increasing number of cycles, represented in a semi-logarithmic plot at the point where the deformation curve begins to concave downwards to indicate a rapid increase in displacement. It is reported by various studies that this critical cyclic stress ratio is between 0.6 and 0.7 (Ansal and Erken, 1989; Miller *et al.,* 2000; Zhou and Gong, 2001). A sinusoidal cyclic load was applied to the specimen under stress-controlled conditions at a frequency of 5 Hz (simulating a 100 km/hr train speed). The applied cyclic amplitude was 25 kPa. The application of cyclic load with PVD was carried out under radial and top drainage in order to simulate the field boundary condition. The tests without PVD were carried out under undrained conditions. Membrane corrections were applied in accordance with ASTM (2002). The axial and volumetric strains were measured using linear variable differential transformers (LVDT). Also, the measurements of excess pore pressures for all test series were at the locations shown in Figure 19a.

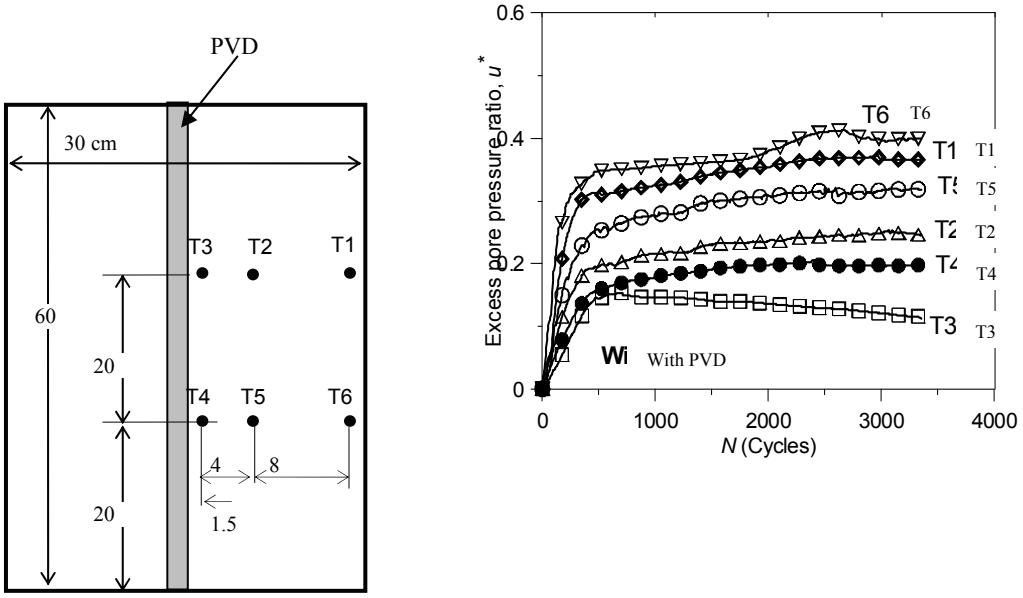

(a) (b)

Figure 19: (a) Locations of the pore pressure transducers at different positions from the PVD inside the soil sample (Indraratna et al., 2009a). (b) Excess pore pressures generated inside the soil sample at different locations from the PVD with the application of cyclic loads (Indraratna *et al.,* 2009a)

4.10.2 Test Results and Analysis

The excess pore water pressure ratio (u^*) is defined as excess pore water pressure normalised to an initial effective pressure (Miller *et al*., 2000, Zhou and Gong, 2001). Figure 19b shows the excess pore pressure ratio (u^*) versus the number of loading cycles (N) under a partially drained condition with PVD. The response of the six transducers shows how the length of the drainage path affects the development of excess water pore pressure. During the application of repeated loads, the PVD significantly reduced the build up of excess pore water pressure and also accelerated dissipation during the rest period. In reality, dissipation of pore water pressure during the rest period will make the track more stable for the next loading (i.e. subsequent passage of train). A soft formation beneath a rail track stabilised by radial drainage (PVD) can be subjected to higher levels of cyclic stress than the critical cyclic stress ratio, without causing undrained failure.

5 FROM THEORY TO PRACTICE: THE USE OF GEOSYNTHETICS AND MATS

5.1 FIELD TESTS ON INSTRUMENTED TRACK AT BULLI

In order to investigate train induced stresses, vertical and lateral track deformations, and the benefits of using geosynthetics, a field trial was carried out on an instrumented track. The University of Wollongong provided technical specifications for the design, while RailCorp (Sydney) provided the funding.

5.1.1 Track Construction

The experimental track section was located between two turnouts in Bulli along RailCorp's South Coast Track, NSW. The total length of the instrumented track section was 60 m. It was divided into four sections, each 15 m long. The layers of ballast and sub-ballast were 300 mm and 150 mm thick, respectively. Fresh and recycled ballast without geosynthetic reinforcement were used at Sections 1 and 4, while the other two sections were built by placing a geocomposite layer between the ballast and sub-ballast (Figure 20).

Figure 20: Installation of geocomposite under the ballast at Bulli, NSW.

5.1.2 Material Specifications

The particle size, gradation, and other index properties of fresh ballast used at the Bulli site were in accordance with the Technical Specification TS 3402 (2001), which represents sharp angular coarse aggregates of crushed latite basalt. Recycled ballast was collected from stockpiles of a recycled plant commissioned by RailCorp at Chullora yard near Sydney. The sub-ballast material was a mixture of sand and gravel. The particle size distribution of fresh ballast, recycled ballast, and sub-ballast (capping) materials used at the instrumented track at Bulli are given in Table 2.

Table 2: Grain size characteristics of ballast and sub-ballast materials (Indraratna *et al*., 2010a)

Material	d_{max} mm	d_{min} mm	d_{50} mm	C_u	C_c
Fresh Ballast	75.0	19.0	35.0	1.5	1.0
Recycled Ballast	75.0	9.5	38.0	1.8	1.0
Sub-ballast	19.0	0.05	0.26	5.0	1.2

Biaxial geogrids were placed over the nonwoven polypropylene geotextiles to serve as the geocomposite layer installed at the ballast-subballast interface. The technical specifications of the geosynthetic material used at this site have been discussed elsewhere by Indraratna *et al*. (2011a).

5.1.3 Track Instrumentation

The performance of each section of track under the repeated loads of moving trains was monitored using sophisticated instrumentation. The vertical and horizontal stresses that would develop in the track bed under repeated wheel loads were measured by pressure cells. Vertical deformations of the track at different sections were measured by settlement pegs and lateral deformations were measured by electronic displacement transducers connected to a computer controlled data acquisition system. The settlement pegs and displacement transducers were installed at the sleeper-ballast and ballast-subballast interfaces, respectively, as shown in Figure 21.

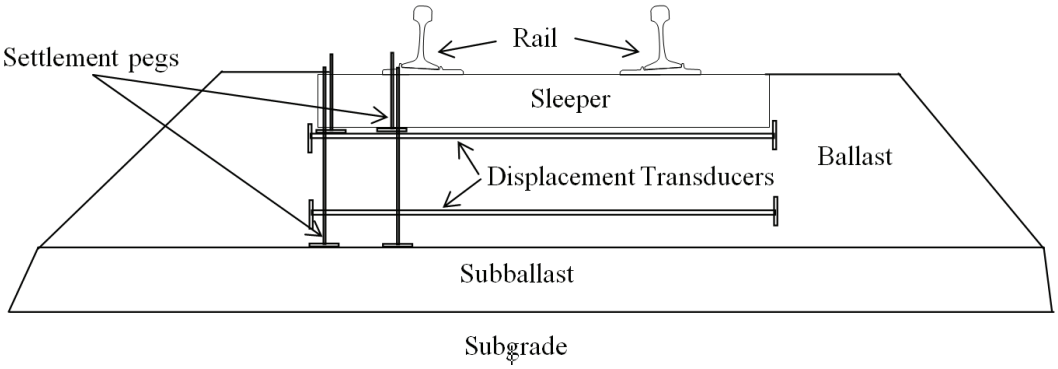

Figure 21: Installation of settlement pegs and displacement transducers at Bulli site.

5.1.4 Ballast deformations

Average ballast deformations are plotted against the number of load cycles (N) in Figure 22. The recycled ballast showed less vertical and lateral deformations because of its moderately graded particle size distribution (C_u = 1.8) compared to the very uniform fresh ballast (C_u = 1.5). Recycled ballast often has less breakage because the individual particles are less angular which prevents corner breakage resulting from high contact stresses. The results presented in Figure 22 indicate that geocomposite reduced vertical deformation of fresh ballast by 33% and that of recycled ballast by 9%. It also reduced lateral deformation of fresh ballast by about 49% and that of recycled ballast by 11%. The apertures of the geogrid offered strong mechanical interlocking with the ballast. The capacity of the ballast to distribute loads was improved by the placement of the geocomposite layer, which substantially reduced settlement under high repeated loading.

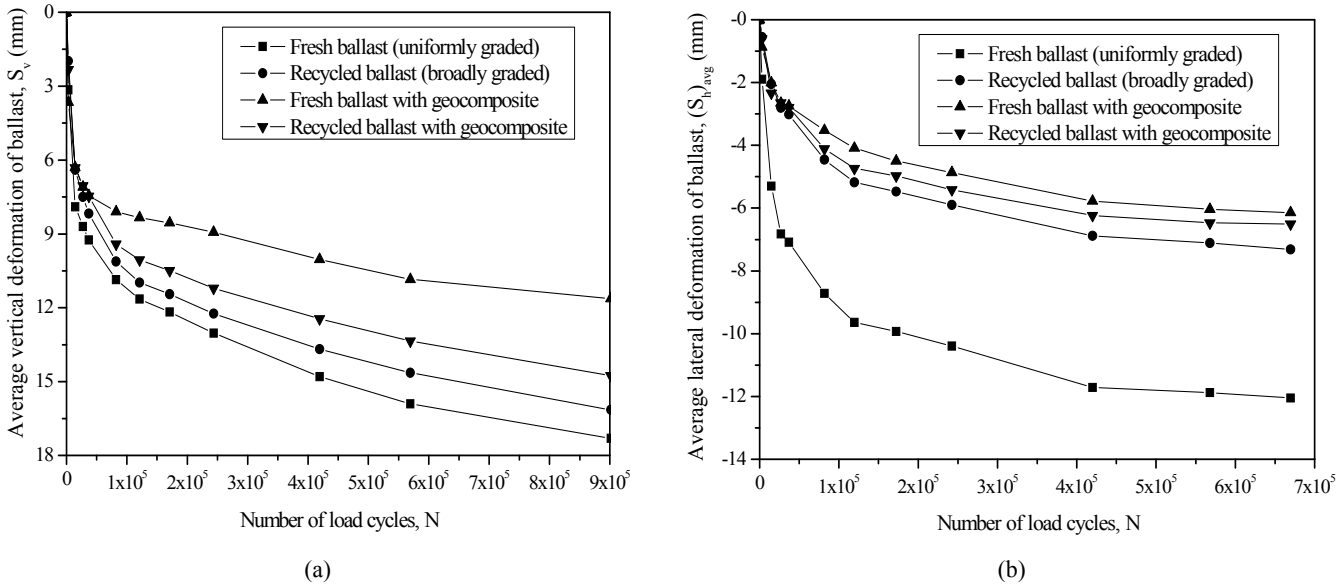

Figure 22: Average deformations of the ballast layer: (a) vertical; (b) lateral (data sourced from Indraratna *et al*., 2010a).

5.1.5 Traffic induced stresses in ballast

Figure 23(a) shows the maximum cyclic vertical (σ_v) and horizontal (σ_h) stresses recorded at Section 1 due to the passage of a coal train with 100-ton wagons (25 tons axle load). The stresses were measured under the rail and at the edge of the sleeper. It is evident that σ_v decreases significantly with depth, while σ_h decreases only marginally with depth

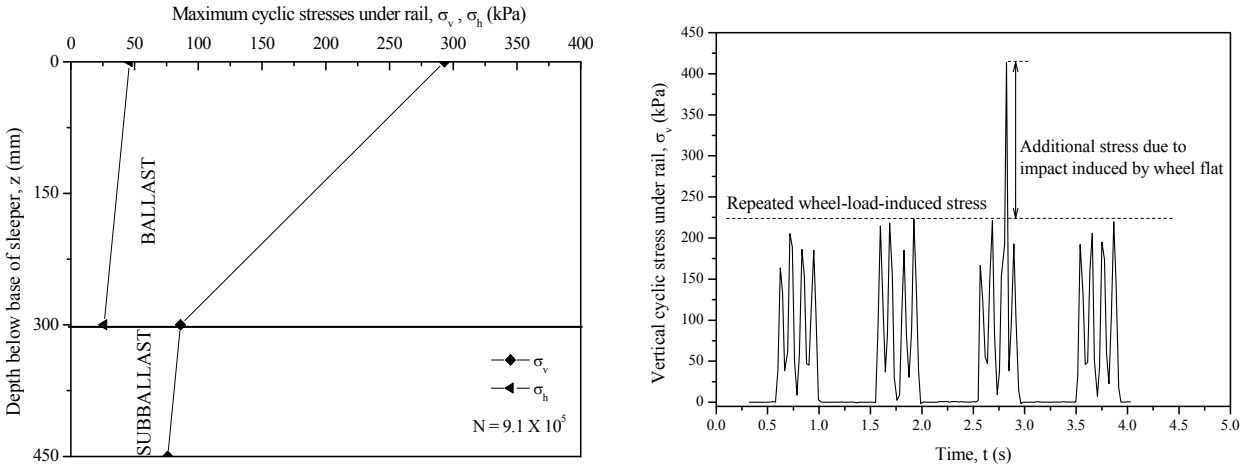

(a) (b)

Figure 23: Cyclic stresses induced by coal train with wagons (100 tons) (data sourced from Indraratna *et al.,* 2010a).

The large vertical stress and relatively small lateral (confining) stress caused large shear strains in the track. Figure 23(b) shows that the peak stress reached 415 kPa, which was associated with a wheel flat. This proved that large dynamic impact stresses can be generated in the ballast by wheel imperfections.

5.2 FIELD TESTS ON INSTRUMENTED TRACK AT SINGLETON

To investigate the performance of different types of geosynthetics to improve overall track stability under *in situ* conditions, an extensive study was undertaken on instrumented track sections near Singleton, NSW, which were part of the Third Track of the Minimbah Bank Stage 1 Line.

5.2.1 Track Construction

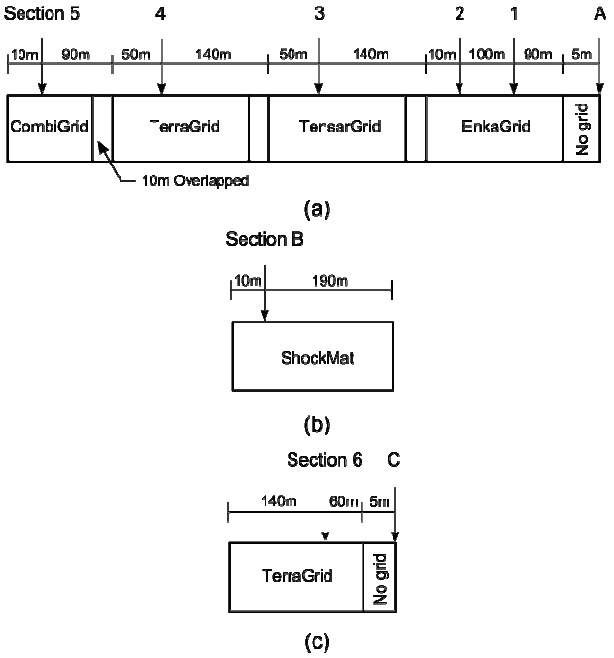

Figure 24: Reinforcement of track substructure with different types of synthetic materials.

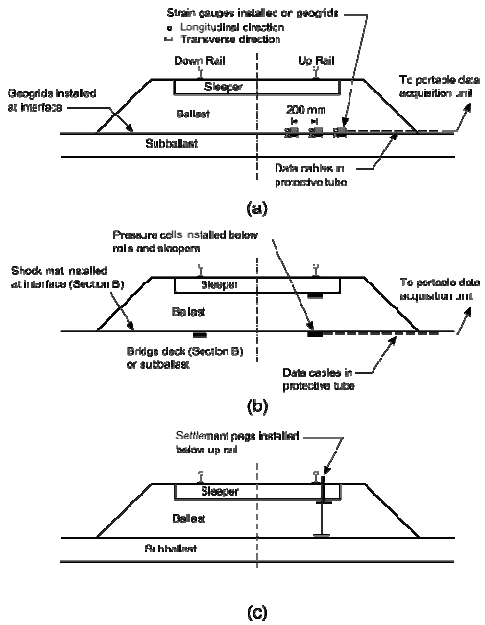

Figure 25: Details of track instrumentation using (a) strain gauges, (b) pressure cells and (c) settlement pegs.

Nine experimental sections were included in the Third Track during the time of track construction on three different types of subgrades including (i) the relatively soft general fill and alluvial silty clay deposit (Sections 1-5 and Section A), (ii) the intermediate cut siltstone (Sections 6 and C) and (iii) the stiff reinforced concrete bridge deck (Section B).

5.2.2 Material Specifications

The track substructure consisted of a 300 mm thick ballast layer (D_{50} = 36 mm, angular latite basalt fragments) underlain by a 150 mm thick sub-ballast layer (GP-GM, compacted sandy gravel, CBR = 50%, D_{50} = 4 mm). A 700 mm thick structural layer of fill (GP-GM, compacted sandy gravel, CBR = 8%, D_{50} = 3 mm) was placed below the sub-ballast layer. Single layers of EnkaGrid, TensarGrid, TerraGrid and CombiGrid (geocomposite) were installed at the ballast-sub-ballast interface (Figures 24a and c). For comparison purposes, no geosynthetic was installed at Sections A and C. A layer of shock mat was installed at the ballast-deck interface at Section B (Figure 24b) to minimise ballast degradation. The properties of the geosynthetics and shock mats used in this study are listed in Table 3.

5.2.3 Track Instrumentation

Strain gauges were used to study the deformations and mobilised forces along the geogrid layers. The strain gauges were a post yield type suitable to measure strains in the range of 0.1 to 15%. The strain gauges were installed in groups, 200 mm apart, and on the top and bottom sides of the grids in both longitudinal and transverse directions (Figure 25a). As shown in Figure 25b, two pressure cells were installed at Sections 1, 6, A and C. At these locations, one pressure cell was installed at the sleeper-ballast and another at the ballast-sub-ballast interface. At Section B however, three pressure cells were installed at the synthetic mat-deck interface. Settlement pegs were also installed at the sleeper-ballast and ballast-sub-ballast interfaces to measure vertical deformations of the ballast layer, as shown in Figure 25c.

Table 3: Mechanical properties of (a) geogrids and geocomposite and (b) synthetic mat.

(a)	Terra Grid	Tensar Grid	Enka Grid	CombiGrid	
Material	Poly ester	Poly ester	Poly ester	Poly propylene (grid)	Poly propylene (fabric)
Type	biaxial	biaxial	biaxial	biaxial	nonwoven
Tensile strength (kN/m)	30/30	30/30	36/36	40/40	6/10
Strain at break (%)	15/15	15/15	15/15	15/15	60/40
Aperture size (mm)	40/40	65/65	44/44	31/31	-
Thickness (mm)	4	3	3	3	2.9

(b)	Shock mat
Material	Polyurethane elastomer
Type	bonded rubber granulates
Particle size (mm)	1-3
Tensile strength (kN/m^2)	600
Strain at break (%)	80
Thickness (mm)	10

5.2.4 Settlement of Ballast

The settlements (S_v) and vertical strains (ε_v) of the ballast layer after 2.3×10^5 load cycles are reported in Table 4. The vertical settlements of sections with reinforcement are generally smaller than those without reinforcement. This phenomenon is mainly attributed to interlocking between the ballast particles and grids, thus creating larger track confinement. When Sections A, B, and C are compared, the results indicate that S_v and ε_v are larger when the subgrade stiffness becomes smaller, i.e. S_v are smallest on the concrete bridge deck and largest at the alluvial deposit.

Table 4: Vertical settlements and strains of ballast layer after 2.3×10^5 load cycles.

	Section								
	1	2	3	4	5	6	A	B	C
Settlement S_v (mm)	16.3	21.2	20.6	14.8	16.0	16.3	23.8	8.8	17.8
Vertical strain ε_v (%)	5.4	7.1	6.9	4.9	5.3	5.4	7.9	2.9	5.9

It is also observed that the ability of geogrid to reduce track settlement becomes higher for softer subgrades. Such an observation is in agreement with the results of full scale tests presented by Ashmawy and Bourdeau (1995). Of the four types of synthetics used, TerraGrid performed most effectively. Although the tensile strength of TerraGrid does not differ much with other types, its aperture size (40 mm) would enable better interlocking between the ballast and grids.

5.2.5 Strains mobilised in Synthetic Grids

Accumulated longitudinal (ε_l) and transverse (ε_t) strains after 2.3×10^5 load cycles are given in Table 5. The transverse strains were generally larger than longitudinal strains, which is attributed to the relative ease for lateral spreading of the ballast. It was also observed that ε_l and ε_t are mainly influenced by deformations of the subgrade. The strains of CombiGrid (Section 5) were relatively large although its higher stiffness could have resulted in smaller strains. This is because the thick general fill underwent large lateral deformations shortly after the track was commissioned. Induced transient strains in both longitudinal and transverse directions due to the passage of trains (axial load of 30 tons) travelling at 40 km/h were of magnitude 0.14-0.17%. Smaller values of ε_{tl} and ε_{tt} were observed in grids with higher stiffness.

Table 5: Accumulated longitudinal and transverse strains in geosynthetics.

	Section					
	1	2	3	4	5	6
Longitudinal strain ε_l (%)	0.80	0.78	0.92	0.61	0.60	0.62
Transverse strain ε_t (%)	0.85	1.50	0.85	0.80	1.80	0.85

6 FROM THEORY TO PRACTICE: APPLICATION OF PREFABRICATED VERTICAL DRAINS (PVDS) UNDER TRAIN LOADS

6.1 SANDGATE TRACK

The Sandgate Rail Grade Separation Project site is located at Sandgate between Maitland and Newcastle, in the Lower Hunter Valley, NSW (Figure 26). Field and laboratory tests were carried out to provide relevant soil parameters. A site investigation included 6 boreholes, 14 piezocone (CPTU) tests, 2 in-situ vane shear tests and 2 test pits. Laboratory tests such as soil index property testing, standard oedometer testing and vane shear testing were also performed. A typical soil profile showed that the thickness of existing soft compressible soil varied from 4 m to 30 m. The soft residual clay is beneath the layer of soft soil and is followed by shale bedrock. The properties of the soil are shown in Figure 27.

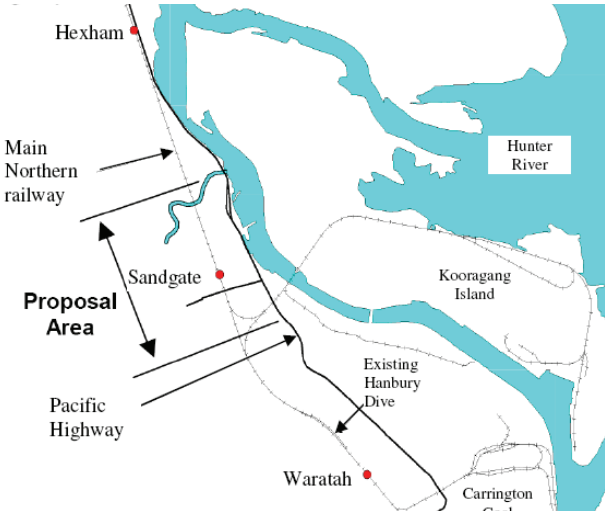

Figure 26: Site location (adopted from Hicks, 2005).

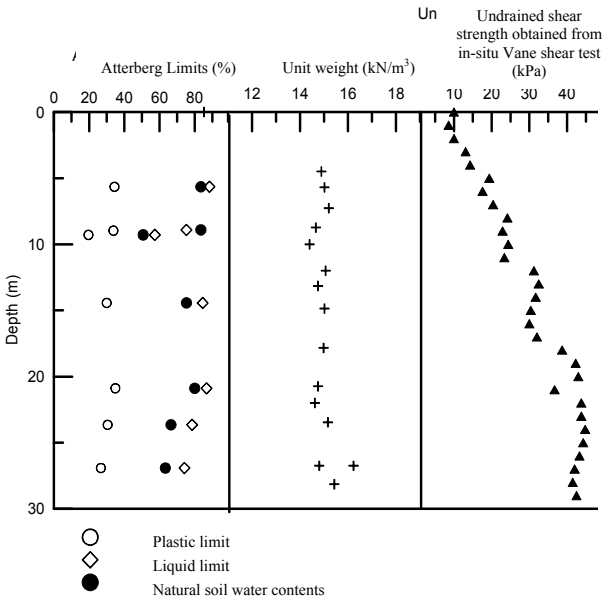

Figure 27: Soil properties at Sandgate Rail Grade Separation Project (Indraratna *et al*., 2010d).

The groundwater level is at the ground surface. The moisture contents of the soil layers were the same as their liquid limits. The soil unit weight varied from 14 kN/m^3 to 16 kN/m^3. The undrained shear strength increased from ~ 10 kPa to 40 kPa. The clay deposit at this site could be considered as lightly over consolidated (OCR ≈ 1-1.2). The horizontal coefficient of consolidation (c_h) is approximately 2-10 times of the vertical coefficient of consolidation (c_v). Based on preliminary numerical analysis conducted by Indraratna *et al*. (2010b), PVDs 8 m in length were suggested and installed in a triangular pattern, 2 m apart. The aims of the field monitoring were to: (a) ensure the stability of the tracks, (b) validate the design of the new railway stabilised by PVDs, and (c) examine the accuracy of the numerical analysis through Class A predictions, where the field measurements were unavailable at the time of finite element modelling.

6.1.1 Preliminary Design

Due to time constraints, rail tracks were built immediately after the PVDs were installed. The train load at very low speed was used as the only external surcharge. The equivalent dynamic loading using an impact load factor was used to predict the settlements and associated excess PWPs. In this analysis, a static pressure of 104 kPa with an impact factor of 1.3 was applied according to the low train speed for axle loads up to 25 ton, based on the Australian Standards AS 1085.14-1997. The over consolidated crust and fill layer was simulated by the Mohr-Coulomb model, whereas the soft clays were conveniently modelled using the Soft Soil model with the finite element code, PLAXIS (Brinkgreve 2002). The soil parameters are given in Table 6. A vertical cross section of mesh discretisation of the formation beneath the rail track is shown in Figure 28. A plane strain finite element analysis employed triangular elements with six displacement nodes and three pore pressure nodes. Four PVDs were used in the analysis. An equivalent plane strain analysis with appropriate conversion from axi-symmetric to 2-D was adopted to analyse the multi-drain analysis (Indraratna *et al*. 2005b). In this method, the corresponding ratio of the smear zone permeability to the undisturbed zone permeability is:

$$\frac{k_{s,ps}}{k_{h,ps}} = \frac{\beta}{k_{h,ps}/k_{h,ax}\left[\ln(n/s) + k_{h,ax}/k_{s,ax}\ln(s) - 0.75\right] - \alpha} \quad \textbf{(4)}$$

$$\alpha = 0.67(n-s)^3/n^2(n-1) \quad \textbf{(4a)}$$

$$\beta = 2(s-1)\left[n(n-s-1)+0.33\left(s^2+s+1\right)\right]/n^2(n-1) \quad \textbf{(4b)}$$

$$n = d_e/d_w \quad \textbf{(4c)}$$

$$s = d_s/d_w \quad \textbf{(4d)}$$

where d_e = the diameter of the unit cell soil cylinder, d_s = the diameter of the smear zone, d_w = the equivalent diameter of the drain, k_s = horizontal soil permeability in the smear zone, k_h = horizontal soil permeability in the undisturbed zone and the top of the drain and subscripts '*ax*' and '*ps*' denote the axisymmetric and plane strain condition, respectively. The ratio of equivalent plane strain to axisymmetric permeability in the undisturbed zone is given by:

$$k_{h,ps}/k_{h,ax} = 0.67(n-1)^2/\left[n^2\left[\ln(n)-0.75\right]\right] \quad \textbf{(5)}$$

Table 6: Selected parameters for soft soil layer used in the FEM (Indraratna *et al*., 2010d).

Soil layer	Depth of layer (m)	Model	c (kPa)	ϕ	e_0	$\lambda/(1+e_0)$	$\kappa/(1+e_0)$	k_v ($\times 10^{-4}$ m/day)	k_h ($\times 10^{-4}$ m/day)
Soft soil-1	1.0-10.0	Soft Soil	10	25	2.26	0.131	0.020	0.70	1.4
Soft soil-2	10.0-20.0	Soft Soil	15	20	2.04	0.141	0.017	0.75	1.5

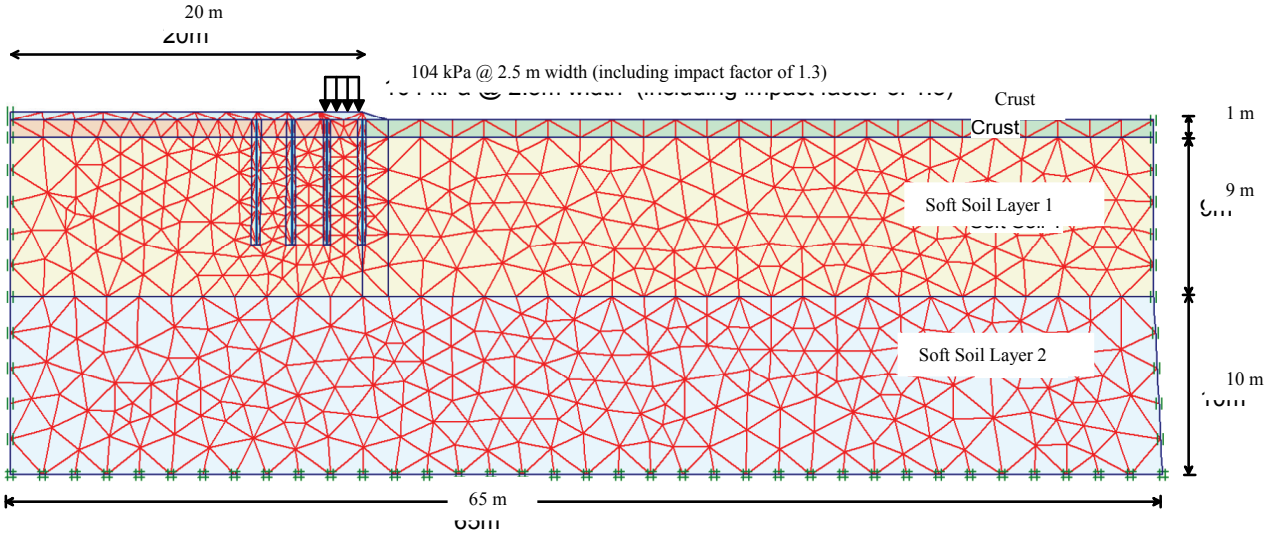

Figure 28: Vertical cross section of rail track and foundation (Indraratna *et al*., 2010d).

6.1.2 Comparison of Field Results with Class A FEM Predictions

The field results were released by the track owner (Australian Rail Track Corporation) a year after the analysis, therefore all predictions can be categorised as Class A (Lambe, 1973). The calculated and observed consolidation settlements at the centre line are presented in Figure 29. The predicted settlement matches very well with the field data for a Class A prediction. The *in situ* lateral displacement at 180 days at the rail embankment toe is illustrated in Figure

30. As expected, maximum displacements are measured within the top clay layer i.e. the softest soil below the 1 m crust. Lateral displacement is restricted to the topmost compacted fill (depth 0-1 m). The Class A predictions of lateral displacements are also in very good agreement with the field behaviour. The effectiveness of wick drains in reducing the effects of undrained cyclic loading through the reduction in lateral movement is evident.

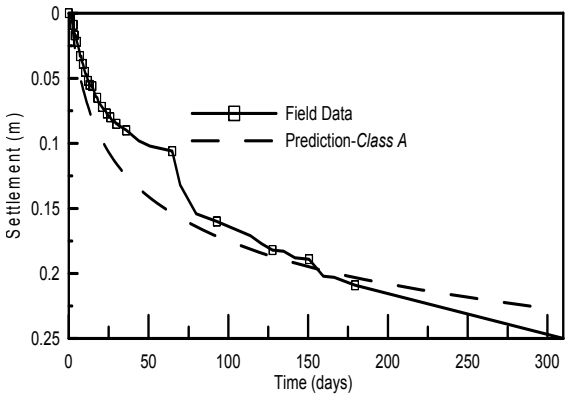

Figure 29: Predicted and measured settlements at the centre line of rail tracks (after Indraratna *et al.,* 2010d)

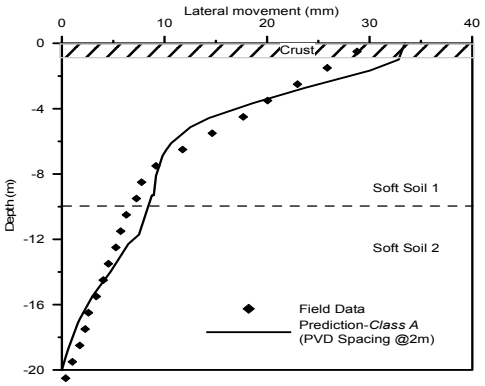

Figure 30: Lateral displacement at the embankment toe at 180 days (after Indraratna *et al.,* 2010d)

7 CONCLUSIONS AND RECOMMENDATIONS

The performance of ballasted rail tracks with geosynthetic reinforcement, shock mats and PVDs, has been discussed through laboratory tests, theoretical modelling, field trials, and numerical simulations. The results highlight that particle breakage, confining pressure, frequency of cyclic loading, soft formation in addition to train loading patterns (cyclic and impact) have a significant influence on the engineering behaviour of ballasted rail track.

The laboratory studies show that permanent deformation and degradation increased with the frequency and number of cycles, but in a 20 Hz $\leq f \leq$ 30 Hz zone, cyclic densification was observed without significant additional ballast breakage. The DEM based micro-mechanical investigation showed that most particles break during the initial cycles, which leads to higher initial axial strains. The detrimental effects of fouling on the shear strength and drainage characteristics were assessed using a new parameter, the Void Contaminant Index (VCI). It was shown that the VCI could accurately capture the fouling of ballast because it could incorporate the effects of void ratios, specific gravities, and gradations of both fouling material and ballast. Initially, even a small increase in the VCI leads to a significant decrease in the hydraulic conductivity of the fouled ballast, but beyond a certain limit of VCI (50% for coal-fouled ballast and 90% for sand-fouled ballast) the hydraulic conductivity converged to that of the fouling materials itself.

The large scale direct shear tests revealed that inclusion of geogrids under ballast layer increased the shear strength of ballast while reducing dilation in the granular assembly because interlocking between the ballast and geogrid increased the peak shear stress associated with increased internal confinement. The lateral deformation of ballast was also reduced by this interlocking effect. However, the benefits gained from the use of geogrid were reduced in coal fouled ballast because the coal fines fill the voids between the ballast particles and coat their surfaces, which decreased inter-particle friction and subsequent resistance to interface shearing. It was also observed that the normalised aperture ratio, (A/D_{50}) had a profound influence on the interface efficiency factor (α). The best size geogrid aperture to optimise the interface shear strength was $1.20D_{50}$. The minimum and maximum sized apertures required to attain the beneficial effects of geogrids were $0.95D_{50}$ and $2.50D_{50}$, respectively. Shock mats at the top and bottom of the ballast bed reduced the impact, irrespective of the type of subgrade. It was also shown that the use of shock mats was beneficial in terms of reduced ballast breakage and attenuated impact forces. The weak subgrade also acts as a flexible cushion. The impact caused the most significant damage to ballast, especially 10 blows caused considerable ballast breakage (BBI = 17%) in case of stiff subgrade. Due to inclusion of shock mat at the top and bottom of the ballast layer, particle breakage was reduced by approximately 47% using a stiff subgrade and by approximately 65% for a weak subgrade. The laboratory investigations on the sub-ballast filter shows that well graded sub-ballast is too porous to effectively capture the fines within its voids. It is recommended that uniformly graded sub-ballast with not more than 30% fine sand (particle range of 0.15 mm - 0.425 mm) have an enhanced filtering capacity. Due to the lack of mechanical resistance against axial deformation, the application of cyclic stress to uniformly graded sub-ballast results in a reduction in porosity that renders the filter more effective in trapping migrating fines.

The 'field' performance of ballasted rail tracks with geosynthetic reinforcement has been discussed in this paper. The performance of instrumented ballasted tracks at Bulli and Singleton was evaluated where different types of ballast and geosynthetic reinforcements were used. The results of the Bulli field study indicated that the use of geocomposites as

reinforcing elements for tracks using recycled ballast proved to be a feasible and effective alternative. According to the results of the Singleton study, the effectiveness of geosynthetics appeared to increase, as the stiffness of subgrade decreased. The strains accumulated in geogrids were influenced by deformation of the subgrade, while the induced transient strains were mainly affected by the stiffness of geogrids. A better understanding of such a performance would allow for safer and more effective design and analysis of ballasted rail tracks with geosynthetic reinforcement. The finite element analysis of the track conducted prior to its construction was considered as a Class A prediction, with continued field monitoring since the time of construction. PVDs significantly decrease the build up of excess pore water pressures (PWP) during cyclic loading and continue to dissipate the excess PWP during the rest period. The dissipation of PWP during the rest period makes the track more stable for the next loading stage. Even with relatively short PVDs, both the predictions and field data proved that lateral displacement can be curtailed. The equivalent plane strain finite element analysis is adequate enough to predict the behaviour of track improved by short PVDs.

8 ACKNOWLEDGEMENTS

The Author wishes to thank the Australia Research Council, CRC for Rail Innovation, RailCorp, ARTC, ARUP, John Holland, Coffey Geotechnics, Queensland Rail National, Douglas Partners, Queensland Transport & Main Roads and BHP Billiton for their continuous support. A number of current and past PhD students, namely Miss Nayoma Tennakoon, Mr Sd K Karimullah Hussaini, Mr Ngoc Trung Ngo, Dr Joanne Lackenby, Dr Daniela Ionescu, Dr Wadud Salim, Dr Dominic Trani and Dr Pramod Kumar Thakur have participated to the contents of this paper and their contributions are greatly acknowledged. The Authors would also like to thank A/Prof Hadi Khabbaz (University of Technology, Sydney), A/Prof Mohamed Shahin (Curtin University of Technology, Perth), Dr Pongpipat Anantanasakul, Dr Jayan Vinod (University of Wollongong, Wollongong). The assistance of Mr David Christie (formerly Senior Geotechnical Consultant, RailCorp), Mr Tim Neville (ARTC), Mr Michael Martin (QR National), Mr Ronald Victor (QR National), Mr Sandy Pfeiffer (RailCorp) and Mr Geoff MacIntosh (Douglas Partners) is gratefully acknowledged. The advice and help over a long period of time by Professor A Balasubramaniam, Griffith University (Qld) is appreciated. A significant portion of the contents have been reproduced with kind permission from the Journal of Geotechnical and Geoenvironmental Engineering ASCE, International Journal of Geomechanics, ASCE, ASTM Geotechnical Testing Journal, Geotechnique, and Canadian Geotechnical Journal.

8 REFERENCES

Altuhafi, F. and Coop, M.R. *Changes to particle characteristics associated with the compression of sands*. Géotechnique, 2011. **61**(6): p. 459-471.

Ansal, A.M. and Erken, A. *Undrained behaviour of clay under cyclic shear stresses*. Journal of Geotechnical Engineering, ASCE, 1989. **115**(7): p. 968-983.

AS 2758.7. *Aggregates and rock for engineering purposes*, Part 7: Railway ballast. Sydney, NSW, Australia, 1996.

Ashmawy, A.K. and Bourdeau, P.L. *Geosynthetic-reinforced soils under repeated loading: a review and comparative design study*. Geosynthetic International, 1995. **2**(4): p. 643-678.

Australia Standards AS 1085.14. *Railway permanent way material*. Sydney, NSW, Australia, 1997.

Australian Standards AS 1289.6.7.3 *Methods of testing soils for engineering purposes - soil strength and consolidation tests* - determination of permeability of a soil - constant head method using a flexible wall permeameter, 1999.

Bergado, D. T., Balasubramanian, A. S., Fannin, R. J. & Holtz, R. D. *Prefabricated vertical drain (PVD) in soft Bangkok clay: a case of NBIA project*. Canadian Geotechnical Journal, 2002. **39**(2): p. 304-315.

Brinkgreve, R.B.J. (2002). *PLAXIS (Version 8) User's Manual*. Delft University of Technology and PLAXIS B.V., Netherlands.

Budiono, D.S., McSweeney, T. and Dhanasekar, M. *The effect of coal dust fouling on the cyclic behaviour of railtrack ballast*, Proceedings of the International Conference on Cyclic Behaviour of Soils and Liquefaction Phenomena, Bochum, Germany, A.A. Balkema, 2004: p. 627-632.

Chang, C. S. *Residual undrained deformation from cyclic loading*. Journal of Geotechnical Engineering Division, ASCE, 1982. **108**(GT4): p. 637-646.

Charles J.A. and Watts K.S. *The influence of confining pressure on the shear strength of compacted rockfill*. Géotechnique, London, U.K., 1980. **30**(4): p. 353-367.

Chrismer, S.M. and Read, D.M. *Examining ballast and subgrade conditions*. Railway Track and Structures, AREA, 1994: p. 39-42.

Dombrow, W., Huang, H. and Tutumluer, E. *Comparison of coal dust fouled railroad ballast behavior-granite vs. limestone*, In E. Tutumluer & I. Al-Qadi (Eds.), Proceedings of Eighth International Conference on the Bearing Capacity of Roads, Railways, and Airfields, London: Taylor and Francis Group, 2009: p. 1349-1357.

Feldman, F. and Nissen, D. *Alternative Testing Method for the Measurement of Ballast Fouling: Percentage Void Contamination*. Conference on Railway Engineering, Wollongong, RTSA, 2002: p. 101-109.

Han, X. and Selig, E.T. *Effects of fouling on ballast settlement*, Proceedings of the Sixth International Heavy Haul Conference, Cape Town, South Africa, 1997: p. 257-268.

Hicks, M. (2005). *Environmental impact statement for the Sandgate Rail Grade Separation*, Hunter Valley Region, Australia.

Holtz, R.D., Jamiolkowski, M., Lancellotta, R. and Pedroni, S. *Prefabricated vertical drains: Design and performance*, CIRIA ground engineering report: Ground improvement, Butterworth- Heinemann, Stoneham, Mass, 1991.

Hossain, Z., Indraratna, B., Darve, F. and Thakur, P. DEM analysis of angular ballast breakage under cyclic loading. Geomechanics and Geoengineering, 2007. **2**(3): p. 175-181.

Indraratna B, Khabbaz H, Salim W., Lackenby J. and Christie D. *Ballast characteristics and the effects of geosynthetics on rail track deformation*. International Conference on Geosynthetics and Geoenvironmental Engineering, ICGGE 2004, Bombay, India: p. 3-12.

Indraratna B. and Redana I.W. *Numerical modeling of vertical drains with smear and well resistance installed in soft clay*. Canadian Geotechnical Journal, 2000. **37**(1): p. 133-145.

Indraratna B. and Salim W. *Deformation and degradation mechanics of recycled ballast- stabilised with geosynthetics*. Soils and Foundations, 2003. **43**(4): p. 35-46

Indraratna B., Hussaini S.K.K. and Vinod JS On the shear behavior of ballast-geosynthetic interfaces, ASTM Geotechnical Testing Journal, 2011b, **35**(2): p. 1-8.

Indraratna B., Ionescu D. and Christie D. *State-of the- art large scale testing of ballast*. Proceedings of Conference on Railway Engineering, CORE2000, 21-23 May, Adelaide, Australia, p. 24.1-24.13.

Indraratna B., Ionescu D. and Christie, D. *Shear behaviour of railway ballast based on large-scale triaxial tests*. Journal of Geotechnical and Geoenvironmental Engineering, ASCE, 1998. **124**(5): p. 439-439.

Indraratna B., Nimbalkar S., Christie D., Rujikiatkamjorn C. and Vinod J. S. *Field Assessment of the Performance of a Ballasted Rail Track with and without Geosynthetics*, Journal of Geotechnical and Geoenvironmental Engineering, ASCE, 2010a. **136**(7): p. 907-917.

Indraratna B., Salim W. and Rujikiatkamjorn, C. *Advanced Rail Geotechnology – Ballasted Track*, CRC Press/Balkema. 2011a.

Indraratna B., Thakur P.K. and Vinod J.S. *Experimental and Numerical Study of Railway Ballast Behaviour under Cyclic Loading*. International Journal of Geomechanics ASCE, 2010b. **10**(4): p. 136-144.

Indraratna B., Wijewardena L.S.S. and Balasubramaniam A.S. *Large-scale testing of greywacke rockfill*. Géotechnique, 1993. **43**(1): p. 37-51.

Indraratna, B. and Nimbalkar, S. *Implications of Ballast Breakage on Ballasted Railway Track based on Numerical Modelling*, Proceedings of 13th International Conference of International Association for Computer Methods and Advances in Computational Mechanics, IACMAG 2011, Australia. p. 1085-1092.

Indraratna, B. and Redana, I. W. *Laboratory determination of smear zone due to vertical drain installation*, Journal of Geotechnical and Geoenvironmental Engineering, ASCE, 1998. **125**(1): 96-99.

Indraratna, B. and Salim, W. *Modeling of particle breakage of coarse aggregates incorporating strength and dilatancy*, Geotechnical Engineering, Proceedings of the Institution of Civil Engineers, London, 2002. **155**(4): p. 243-252.

Indraratna, B., Attya, A. and Rujikiatkamjorn, C. *Experimental Investigation on effectiveness of a vertical drain under cyclic loads*. Journal of Geotechnical and Geoenvironmental Engineering, ASCE, 2009a. **135**(6): p. 835-839.

Indraratna, B., Balasubramaniam, A. and Balachandran, S. *Performance of test embankment constructed to failure on soft marine clay*. Journal of Geotechnical Engineering, ASCE, 1992. **118**(1): p.12-33.

Indraratna, B., Ionescu, D., Christie, D. and Chowdhury, R. *Compression and Degradation of Railway Ballast under One-dimensional Consolidation*. Australian Geomechanics Journal, 1997. p. 48-61.

Indraratna, B., Lackenby, J. and Christie, D. *Effect of confining pressure on the degradation of ballast under cyclic loading*. Geotechnique, 2005. **55**(4): p. 325-328.

Indraratna, B., Ngo, N.T. and Rujikiatkamjorn, C. *Behavior of geogrid-reinforced ballast under various levels of fouling*, Geotextiles and Geomembranes, 2011c. **29**: p. 311-322.

Indraratna, B., Nimbalkar, S. and Rujikiatkamjorn, C. *Use of Geosynthetics in Railways including Geocomposites and Vertical Drains*, Geo-frontiers 2011, Advances in Geotechnical Engineering, ASCE Annual GI Conference, Dallas, Texas, USA, 2011d: p. 4733-4742.

Indraratna, B., Nimbalkar, S. and Tennakoon, N. *The behaviour of ballasted track foundations: track drainage and geosynthetic reinforcement*, GeoFlorida 2010, ASCE Annual GI Conference, February 20-24, 2010, West Palm Beach, Florida, USA, 2010c: p. 2378-2387.

Indraratna, B., Nimbalkar, S., Rujikiatkamjorn, C. and Christie, D. *State-of-the-art design aspects of ballasted rail tracks incorporating particle breakage, role of confining pressure and geosynthetic reinforcement*. Proceedings of 9th World Congress on Railway Research, WCRR 2011, Lille, France, 2011e: p. 1-13.

Indraratna, B., Rujikiatkamjorn, C. and Sathananthan, I. *Analytical and numerical solutions for a single vertical drain including the effects of vacuum preloading*. Canadian Geotechnical Journal, 2005b. **42**: p. 994-1014.

Indraratna, B., Rujikiatkamjorn, C., Ewers, B. and Adams, M. *Class A prediction of the behaviour of soft estuarine soil foundation stabilised by short vertical drains beneath a rail track*. Journal of Geotechnical and Geoenvironmental Engineering, ASCE, 2010d. **136**(5): p. 686-696.

Infrastructure Australia. *Better Infrastructure Decision Making Guidelines*, Templates for Stage 7, Sydney, 2010.

Jenkins, H.M., Stephenson, J.E., Clayton, G.A., Morland, J. W. and Lyon, D. *The effect of track and vehicle parameters on wheel/rail vertical dynamic forces*. Railway Engineering Journal, 1974. **3**: p. 2-16.

Kaewunruen, S. and Remennikov, A. *Dynamic crack propagations in prestressed concrete sleepers in railway track systems subjected to severe impact loads*. Journal of Structural Engineering, ASCE, 2010, **136**(6): p. 749-754.

Lackenby, J., Indraratna, B. and McDowel, G. *The role of confining pressure on cyclic triaxial behaviour of ballast*. Geotechnique, 2007. **57**(6): p. 527-536.

Lambe, T.W. *Predictions in soil engineering*. Geotechnique, 1973. **23**: p. 149-202.

Locke, M., Indraratna, B. and Adikari G. *Time-dependent particle transport through granular filters*. Journal of Geotechnical and Geoenvironmental Engineering, ASCE, 2001. **127**(6): p.521-529.

Luo, Y., Yin, H. and Hua, C. *Dynamic response of railway ballast to the action of trains moving at different speeds*. Proceedings of the Institution of Mechanical Engineers, Part F: Journal of Rail and Rapid Transit, 1996. **210**(2): p. 95-101.

Marachi N.D., Chan C.K. and Seed H.B., *Evaluation of properties of rockfill materials*. Journal of the Soil Mechanics and Foundations Division, ASCE, 1972. **96**(6): p. 95-114.

Marsal, R.J. *Mechanical properties of rock fill*. In: Hirschfield R. C. and Pools, S. J. (eds) Embankment Dam Engineering: Casagrande Volume, Wiley, New York, 1973: p. 109-200.

Miller, G.A., Teh, S.Y., Li, D. and Zaman, M.M. *Cyclic shear strength of soft railroad subgrade*. Journal of Geotechnical and Geoenvironmental Engineering, ASCE, 2000. **126**(2): p. 139-147.

Mohamedelhassan E. and Shang, J.Q. *Vacuum and surcharge combined one-dimensional consolidation of clay soils*, Canadian Geotechnical Journal, 2002. **39**(5): p. 1126-1138.

Nimbalkar, S., Indraratna, B., Dash, S.K. and Christie, D. *Improved performance of railway ballast under impact loads using shock mats*. Journal of Geotechnical and Geoenvironmental Engineering, ASCE, 2012. 138(3): 281-294.

PLAXIS. *PLAXIS 2D Version 8.6 - Finite element code for soil and rock analysis*. Delft, The Netherlands: A. A. Balkema Publishers, 2007.

Ramamurthy T. *Shear strength response of some geological materials in triaxial compression*. International Journal of Rock Mechanics and Mining Sciences, 2001. **38**: p. 683-697.

Raymond, G.P. and Davies, J.R. *Triaxial tests on dolomite railroad ballast*. Journal of Geotechnical Engineering Division, ASCE, 1978. **104**(GT6): p. 737-751.

Raymond, G.P. *Reinforced ballast behaviour subjected to repeated load*. Geotextiles and Geomembranes, 2002. **20**(1): p. 39-61.

Salim, W. and Indraratna, B. *A New elasto-plastic constitutive model for granular aggregates incorporating particle breakage*, Canadian Geotechnical Journal, 2004. **41**(4); p. 657-671.

Schanz, T., Vermeer, P.A. and Bonnier, P.G. *The Hardening Soil Model - Formulation and Verification*, Proceedings of Plaxis Symposium Beyond 2000 in Computational Geotechnics, Balkema, Rotterdam 1999: p. 55-58.

Selig, E.T. and Waters, J.M. *Track Geotechnology and Substructure Management*, Thomas Telford, London. 1994.

T. S. 3402. *Specification for Supply of Aggregates for Ballast*. Rail Infrastructure Corporation of NSW, Sydney, Australia, 2001.

Tennakoon, N., Indraratna, B., Rujikiatkamjorn, C., Nimbalkar, S. and Neville, T. *The role of ballast fouling characteristics on the drainage capacity of rail substructure*, ASTM Geotechnical Testing Journal (in press), 2012.

Trani, L.D.O. and Indraratna, B. *Experimental investigations into subballast filtration behavior under cyclic conditions*. Australian Geomechanics Society Journal, 2010b. **45**(3): p. 123-133.

Trani, L.D.O. and Indraratna, B. *The use of impedance probe for estimation of porosity changes in saturated granular filters under cyclic loading: calibration and application*. Journal of Geotechnical and Geoenvironmental Engineering, ASCE, 2010c. **136**(10): p. 1469-1474.

Trani, L.D.O. and Indraratna, B.*Assessment of subballast filtration under cyclic loading*. Journal of Geotechnical and Geoenvironmental Engineering, 2010a. **136**(11): p.1519-1528.

Tutumluer, E., Dombrow, W. and Huang, H. *Laboratory characterization of coal dust fouled ballast*, In Proceedings of the AREMA 2008 Annual Conference and Exposition, 21-24 September 2008, Salt Lake City, Utah. American Railway Engineering and Maintenance-of-Way Association, Lanham, 2008: p. 93-101.

Zhou, J. and Gong, X. *Strain degradation of saturated clay under cyclic loading*. Canadian Geotechnical Journal, 2001. **38**: p. 208-212.